



Intriguing minerals: quartz and its polymorphic modifications

Gligor Jovanovski¹ · Tena Šijakova-Ivanova² · Ivan Boev² · Blažo Boev² · Petre Makreski³

Received: 5 November 2021 / Accepted: 21 January 2022
© The Author(s), under exclusive licence to Springer Nature Switzerland AG 2022

Abstract

This lecture text condenses the characteristics of quartz and its rich palette of varieties. The mineralogy and crystallography of quartz and its forms, the origin of its colors, and their important physical and chemical characteristics are discussed. The geological occurrence of quartz and its varieties in the world is also presented, with special attention to North Macedonia. Their applications in various industries are also included. Knowledge of the specific properties of SiO₂ minerals is indispensable for understanding and reconstruction of geological processes, as well as for specific technical applications.

Keywords Quartz · Tridymite · Cristobalite · Rock crystal · Smoky quartz · Amethyst · Chalcedony · Agate · Opal

Introduction

Quartz is a very abundant mineral known as one of the most common minerals found in the Earth's crust [1]. This chemical compound consists of silicon and oxygen atoms, being commonly known as silicon dioxide (SiO₂), also referred to as silica. It can be found in many different geological environments, and its visual appearance reflects the various conditions under which it was formed. Large parts of the Earth's surface are literally covered by quartz—sand left over from the weathering of rocks, due to its great physical and chemical resistance. Along with calcite, quartz is one of the few minerals that together almost entirely compose quartzite and sandstone rocks, but its richest presence is found in granites and related rocks. The various modifications of silica, especially quartz, play a central role in the composition of geological materials. In addition, quartz is

widely used as a raw material in numerous industrial fields. Therefore, knowledge of the specific properties of SiO₂ rocks and minerals is indispensable for the understanding and reconstruction of geological processes, as well as for specific technical applications.

Here, an overview of the basic mineralogical, physico-chemical, and structural characteristics of quartz and its polymorphic modifications is presented. The world localities of their appearance and their practical uses are also discussed.

Origin of name

The most ancient Greek name *κρύσταλλος* (*kristallos*) referring to quartz is mentioned by Theophrastus (ca. 371–ca. 287 BC, the pupil and successor of Aristotle) in his book of stones [2]. The root words *κρύος* meaning “ice cold” and *στέλλειν* meaning “to contract (or solidify)” suggest the ancient belief that *kristallos* was supercooled (permanently solidified) ice [3].

The earliest printed use of “querz” was published anonymously, probably in 1505, and attributed to a physician in Freiberg, Germany, Ulrich Rühle von Kalbe (von Calw) (1465–1523) [3]. Georgius Agricola (1494–1555) used the spelling “quarzum” [4] as well as “querze,” but also referred to “crystallum,” “silicum,” “silex,” and “silice.” Later, the name “quartz” appeared in two English books in 1685 and 1725 [5, 6]. The etymology of the word “quartz” is still under debate, with some linguists tracing it back to Slavic [7] but others to German terms [8].

✉ Gligor Jovanovski
gligor@pmf.ukim.mk

✉ Petre Makreski
petremak@pmf.ukim.mk

¹ Research Center for Environment and Materials, Academy of Sciences and Arts of North Macedonia, MASA, Bul. Krste Misirkov 2, 1000 Skopje, North Macedonia

² Faculty of Natural and Technical Sciences, Goce Delčev University, Štip, North Macedonia

³ Institute of Chemistry, Faculty of Natural Sciences and Mathematics, Ss Cyril and Methodius University in Skopje, Arhimedova 5, 1000 Skopje, North Macedonia

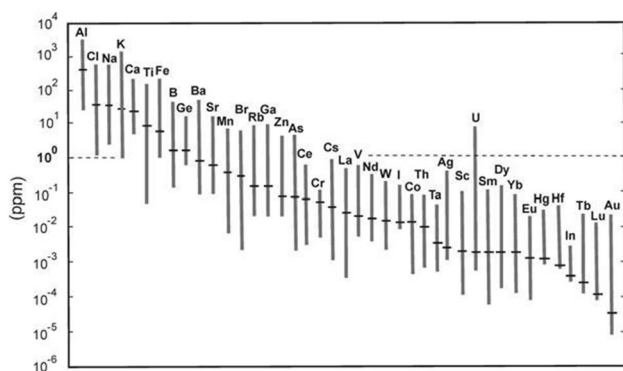


Fig. 1 Average abundance and variations of trace elements in quartz [14] (reprinted with permission from Cambridge University Press)

Mineralogical classification

According to the New Dana Classification of mineral species [9], quartz belongs to the primary group of “(75) tectosilicates Si tetrahedral frameworks, further classified under the subgroup “(75.01) Si Tetrahedral Frameworks—SiO₂ with [four] coordinated Si,” and further categorized to (75.1.3.1). In this latter division, quartz is joined by cristobalite (75.1.1.1), tridymite (75.1.2.1), coesite (75.1.4.1), and seifertite (75.1.6). In the Nickel–Strunz¹ classification [10], quartz (04.DA.05) is found in “04 Oxides (hydroxides, V[five,six] vanadates, arsenites, antimonites, bismuthites, sulfites, selenites, tellurites, iodates),” than fits into the subgroup “04.D metal:oxygen = 1:2 and similar,” and is finally classified into the tertiary group 04.DA. Also, according to Hey’s Chemical Index² of minerals [11], quartz (7.8.1) is also in the “(7) oxides and hydroxides” group, and in particular in the “(8) oxides” subgroup.

Chemical formula and trace elements in quartz

Quartz consists of silicon (46.74 mass %) and oxygen (53.26 mass %), corresponding to the chemical formula SiO₂.

Quartz is one of the purest minerals in the Earth’s crust. Impurities in the form of trace elements can be either incorporated into the crystal structure or bound to microinclusions (fluid or mineral inclusions). Figure 1 illustrates that few elements are present in quartz in concentrations > 1 ppm.

¹ Named after the German mineralogist Karl Hugo Strunz (1910–2006), who introduced a new mineral classification in 1941, later published together with the Canadian mineralogist Ernest Henry Nickel (1925–2009).

² Named after the British mineralogist Max H. Hey (1904–1984).

This is due to the limited number of ions that can substitute for Si⁴⁺ in the crystal lattice. Structural incorporation at a regular Si⁴⁺ lattice position has been proved for Al³⁺, Ga³⁺, Fe³⁺, Ge⁴⁺, Ti⁴⁺, and P⁵⁺ [12, 13]. The average incorporation of trace elements in quartz is presented in Fig. 1 [14].

Silica polymorphs

The silica minerals, with overall composition SiO₂, include many polymorphs [14]. Quartz is the most common member, occurring in both a low-temperature, trigonal system known as α-quartz and a high-temperature hexagonal system known as β-quartz. Other important silica polymorphs are α- and β-tridymite, α- and β-cristobalite, coesite, and stishovite. Opal is an amorphous solid silica containing a large amount of water.

When silica crystallizes (due to the slow cooling of molten rock, the slow cooling of hot silica-rich water, or the evaporation of such a solution) below 573 °C, the crystalline phase is referred as “low quartz.” If the formation occurs within the temperature range of 573–870 °C at normal pressure, the crystalline phase is known as “high quartz.” The crystalline phase formed in the temperature range of 870–1470 °C is known as “tridymite,” while that formed at temperatures in the interval from 1470 to 1720 °C it is known as “cristobalite.” If high quartz is cooled below 573 °C, it transforms rapidly into low quartz, and the reverse solid–solid transformation occurs when low quartz is heated above 573 °C.

At the transition temperature, β-quartz’s tetrahedral framework twists, resulting in the symmetry of α-quartz. At temperatures above 867 °C, β-quartz transforms into tridymite, but this alteration is slower because chemical bonds are broken to form a more open structure. At high pressure, α-quartz transforms into coesite, and at very higher pressures into stishovite. The stability fields of some silica polymorphs are shown in Fig. 2.

Moganite is also considered a polymorph of quartz. When heated above 900 °C, moganite and chalcedony reconstructively transform into cristobalite with moderate stacking disorder. Below 900 °C, moganite does not show any phase transition [16].

Quartz morphology, crystal habits, and twinning

Quartz appears in the form of individual crystals or crystal aggregates. Often, it occurs in anhedral granular masses, in cryptocrystalline or rolled grains. Quartz commonly appears in prismatic crystals with unequally developed rhombohedral terminations [17–20].

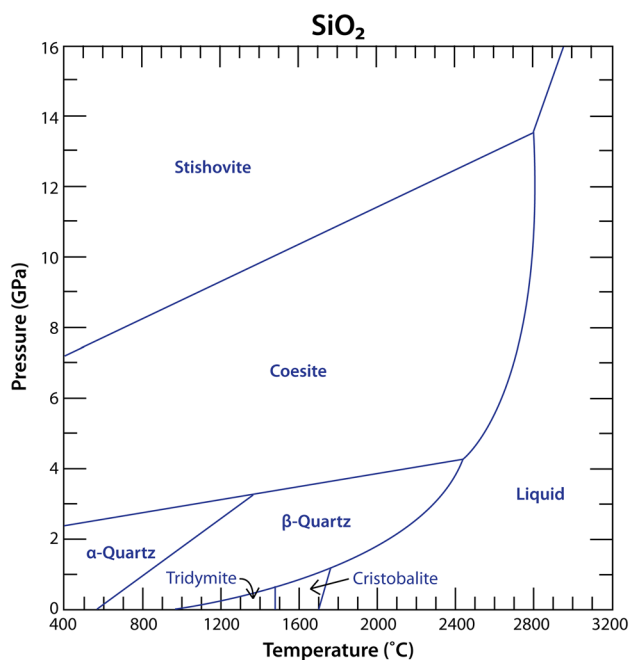


Fig. 2 Phase diagram for the silica system [15] (Credit: Pamela Burnley, University of Nevada-Las Vegas, <https://creativecommons.org/licenses/by-nc-sa/3.0/>)

The prism faces are horizontally striated. Right- and left-handedness can only be determined macroscopically when $\{11\bar{2}1\}$ is present. This face lies to the right of $\{10\bar{1}0\}$, which is below the larger rhombohedron $\{10\bar{1}1\}$ in a right-handed crystal but to the left of $\{10\bar{1}0\}$ in a left-handed crystal. Striations on $\{11\bar{2}1\}$ are parallel to the edge $\{10\bar{1}0\}/\{0010\}$ (Fig. 3).

The term “habit” is used to designate the overall shape of individual crystals, regardless of their crystallographic form (crystal faces). Confusingly, the definitions of some habits of quartz crystals do include specific forms. Many of the trivial names of these habits have been introduced and popularized by rockhounds in the Alps [21, 22]. The most important habits are shown in Fig. 4.

Two types of common twins are observed, where twinning is often not externally manifested: Dauphiné law twins and Brazil law twins [24].

The Dauphiné twin (also called the Swiss law twin or Alpine law twin) is an interpenetrant twin type along the $[0001]$ twin axis. Thereby, all axes in the two parts are parallel [25] (Fig. 5).

The Brazil law is an interpenetrant twinning of left- and right-handed crystal along the twin plane $\{11\bar{2}0\}$ [26] (Fig. 5). Very rarely, crystals can show a special type of twinning of Dauphiné and Brazil law domains in one crystal, being called the Liebisch law, Dauphiné–Brazil law, or Leydolt law [27].

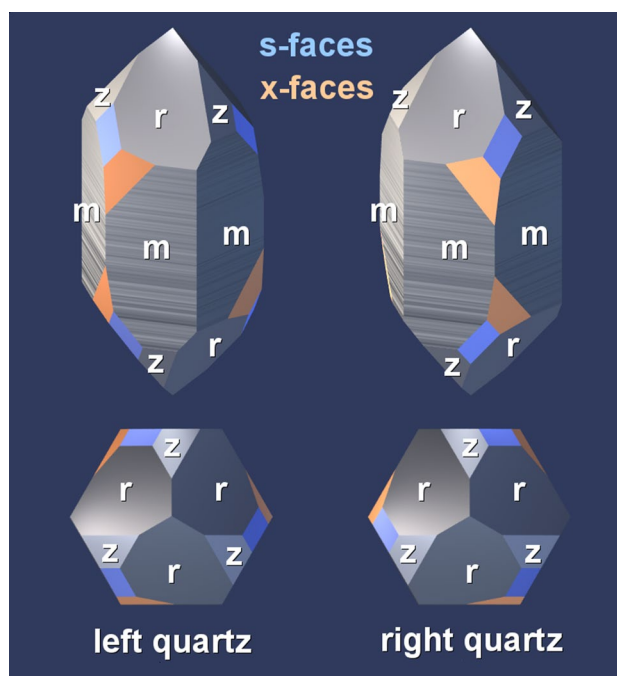


Fig. 3 As- and x-faces on left- and right-handed quartz (*m*: six faces belonging to the central six-sided prism with a typical horizontal striation; *r*: three, often roughly triangular faces at the crystal’s tips; in well-developed crystals these faces are always present; *z*: three, often triangular faces also at the crystal’s tips, which sit between the *r* faces; *s*-faces are a rhomb; *x*-faces are usually either a triangle or—when bordering an *s*-face—a trapezoid) [19] (with kind permission from Dr. Amir C. Akhavan)

Other twins with inclined main axes also exist and are known as Japanese law twins [28]. These are contact twins with the twinning plane $\{11\bar{2}2\}$ [29]. The *c*-axes of the two crystals meet at an angle of $84^\circ 33'$ (Fig. 5). Twinning on the plane $\{10\bar{1}1\}$ may also appear. The twin laws are named after localities where such specimens were first found.

Crystalline quartz samples showing Brazil, Dauphiné, and Japanese twins are presented in Figs. 6, 7, and 8, respectively. More detailed information and images of these three types of twinning in quartz are given in Refs. [31–33].

Structure of quartz and the nature of the Si–O bond

α -Quartz (low quartz) crystallizes in a trigonal crystal system, again with either a right- or left-handed symmetry group: crystal class 32, space group $P3_121$ (left) or $P3_221$ (right), $Z=3$ [34]. The β -quartz (high quartz) structure is hexagonal, with either left- or right-handed symmetry groups, which are equally populated in crystals: crystal class 622, space group $P6_222$ or $P6_422$, $Z=3$ [35]. The unit cell parameters are $a=4.9133 \text{ \AA}$ and $c=5.4053 \text{ \AA}$. The direct

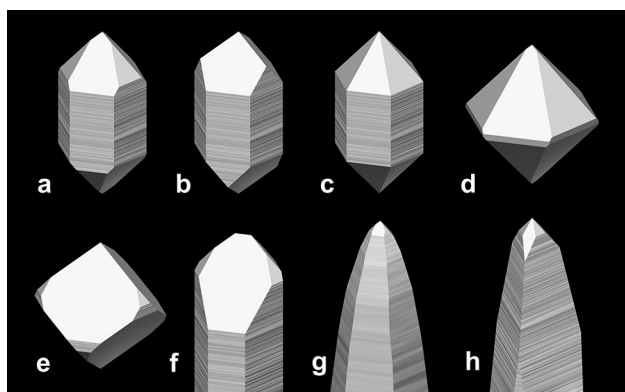


Fig. 4 Common habits of quartz crystals: **a** *normal habit*, typical quartz crystals that are not or are only slightly tapered; **b** *trigonal habit*, crystals with obvious trigonal symmetry, for example, because of missing z faces, or because of a triangular cross-section; **c** *pseudohexagonal habit*, crystals with even development of rhombohedral and prism faces; **d** *Cumberland habit*, crystals with very small or absent prism faces, often bipyramidal; **e** *pseudocubic quartz*, crystals with dominant r or z faces that look like slightly distorted cubes; **f** *Dauphiné habit*, crystal tips with a single very dominant rhombohedral face; **g** *Tessin habit*, crystals that are tapered by steep rhombohedral faces $\{h0\bar{1}1\}$ in the strict sense being dominated by $\{30\bar{3}1\}$ faces. At the original locality, they possess a macromosaic structure; **h** *Muzo habit*, crystals with prism faces that are tapered under the z faces because these are made of a succession of alternating m and z faces, and they have a trigonal cross section at the crystal tips [23] (with kind permission from Dr. Amir C. Akhavan)

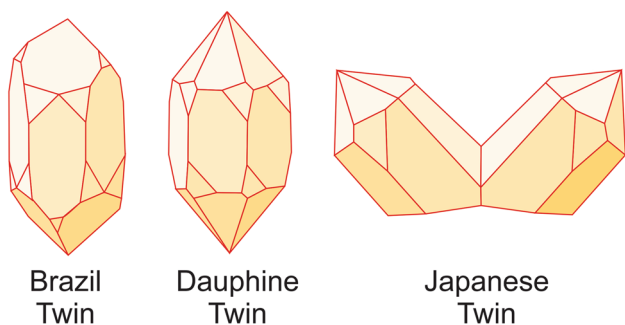


Fig. 5 Schematic presentation of three types of twinning of quartz: Brazil twin $\{11\bar{2}0\}$, Dauphiné twin $[0001]$, and Japanese twin $\{11\bar{2}2\}$ [30] (Credit: OpenGeology, Free Open Educational Resources for the Geosciences, <https://creativecommons.org/licenses/by-nc-sa/4.0/>)

and reverse α - to β -quartz transformation involves only a minor rotation of the SiO_4 tetrahedra with respect to one another [36]. Thereby, no changes in their linking pattern occur.

The basic structural building block is the SiO_4 group, in which four oxygen atoms surround a central silicon atom to form a tetrahedron. Since each oxygen atom is shared by two SiO_4 groups, the formula of quartz is SiO_2 . Covalent bonds are dominant in this structure, and the whole crystal

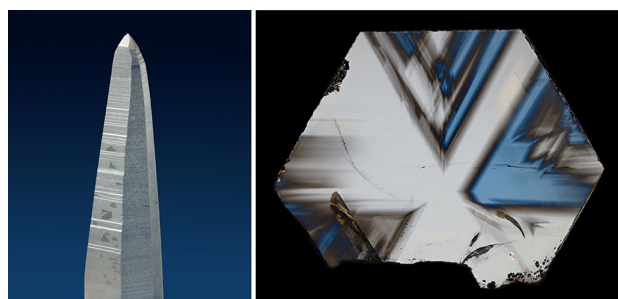


Fig. 6 Quartz Brazil twins. (left) Quartz crystal from Joaquim Felício, Minas Gerais, Brazil [31]. (right) Cross section of a Herkimer diamond (from Middleville, New York), showing twin domains in polarized light. The image corresponds to the triangular patterns of the prism surface. (With kind permission from Dr. Amir C. Akhavan)



Fig. 7 Smoky quartz Dauphiné twin from Val Giuv Valley, Graubünden, Switzerland [32] (with kind permission from Dr. Amir C. Akhavan)



Fig. 8 Quartz (var. amethyst) Japanese twin from Piedra Parada (Piedras Parado), Municipio de Tatatila, Veracruz, Mexico [33] (with kind permission from Rob Lavinsky)

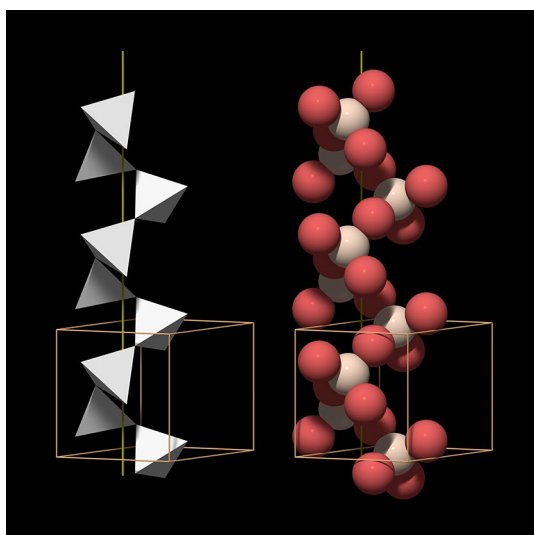


Fig. 9 Threefold helix made of SiO_4 groups [38] (with kind permission from Dr. Amir C. Akhavan)

can be considered to be one large molecule. Silicon and oxygen atoms bond alternately to form infinite chains along the crystallographic c -axis. The SiO_4 tetrahedra form a three-dimensional network, and many mineralogy textbooks classify quartz as a framework silicate or tectosilicate. Quartz can be considered as being made of three- and sixfold helical chains of SiO_4 tetrahedra that run parallel to the c -axis. Two representations of a threefold SiO_4 helix and its relationship to the quartz unit cell are shown in Fig. 9. On the left side, a tetrahedral model is shown, with the corners of the tetrahedra at the position of the oxygen atoms, while on the right side, a ball model with red oxygen and white silicon atoms is presented. Six such helices are connected to form a ring that surrounds a central channel running parallel to the c -axis, sometimes called the “ c -channel.” The SiO_4 tetrahedra around the central c -channel form two independent sixfold helices. Figure 10 shows two views of the corresponding structure: (top) looking in the direction of the c -axis and (bottom) looking in the direction of the a -axis. Like quartz crystals, the ring is six-sided but has trigonal symmetry. The large channels are an important structural feature of quartz because they may be occupied by small cations.

The structure of quartz is more complex compared with that of either tridymite or cristobalite. In tridymite, SiO_4 tetrahedra are packed in a two-layered structure, whereas the structure of cristobalite consists of three layers [37]. Cristobalite has a diamond-type structure where silicon atoms (substituting carbon atoms in the diamond lattice) are bridged by oxygens. On the other hand, tridymite has a wurtzite-type structure.

An important chemical aspect is related to the character of the Si–O bonding in quartz. In this regard, a plethora of

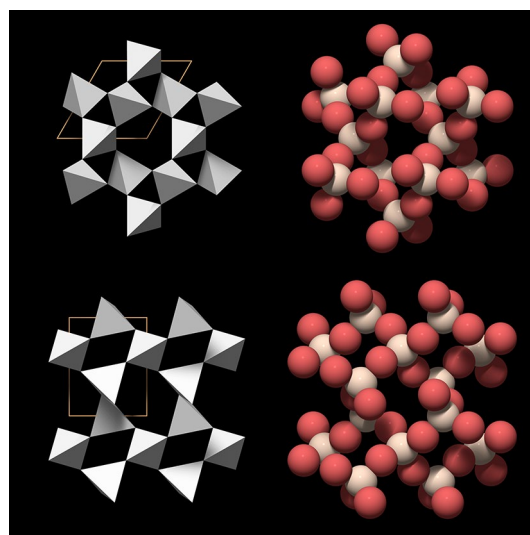


Fig. 10 Basic structural features of quartz [39] (with kind permission from Dr. Amir C. Akhavan)

detailed studies on silicates have been reported to elucidate the nature of the bond, but no convergence to a uniform consensus on whether it is ionic or covalent has been reached. Gibbs et al. [40] provide a detailed comprehensive review on this matter, reflecting on the studies of Smyth [41], Cohen [42], Prencipe et al. [43], and Prencipe and Nestola [44] that report in favor of a largely ionic bond. These authors [40] also pinpointed the influential works of Harrison [45] and Stewart et al. [46] that opt for a predominantly covalent bond, but also outlined their study [47] in line with the work of Pauling [48] that supports an intermediate (between ionic and covalent) character for the Si–O bond. When quartz is considered as a fully ionic compound, consisting of Si^{+4} and O^{-2} , a reasonably good fit to the dielectric properties and cohesive energy was outlined [49–51]. The intermediate model with Si^{+2} and O^{-1} ions provides a better fit to the photon frequencies and to Phillip’s [52] dielectric model [50, 53]. A covalent model with residual charges of +1 on Si and -0.5 e.u. is consistent with the electron density (ED) distribution observed for quartz [46].

At a molecular level, many studies have focused on elucidating the reactions of silicon atoms with oxygen to yield solid SiO_2 [54–56]. However, the theoretical investigation of the reactions of silicon atoms with oxygen barely report on the SiO_2 energy hypersurface. This consideration yields a linear OSiO molecule with the minimum energy within the series of SiO_2 isomers. The thermodynamic data reveal an exothermic reaction and the possibility for formation of SiO when splitting molecular oxygen (from SiO_2) into two atoms and recombination of one of them with a silicon atom [56]. Therefore, one might expect the formation of either OSiO or SiO upon reaction of silicon atoms with oxygen

(oxidation), which is in agreement with experiment. Namely, SiO is dominantly formed after codeposition of Si atoms and molecular oxygen (in argon at 10 K), while a small fraction of SiO₂ is produced along with traces of O₃ (the latter resulting from the combination of molecular oxygen and O atoms) [56].

Macroscopic structure of quartz crystals

Quartz crystals may develop two very distinct types of internal structural compartmentation, viz. lamellar and macro-mosaic structure.

The lamellar structure was first described by Weil [57]. Such crystals consist of layers and show a biaxial optical anomaly. The layers are stacked parallel to the crystal faces in an onion-like manner and are associated with relatively high hydrogen and aluminum content [57–59]. Lamellar quartz cannot be safely recognized without studying the optical properties of the crystal in a thin section. These crystals are sometimes called “Bambauer quartz.” In specimens from Madagascar [57], the lamellar structure was found in the outer parts of the crystal. A study of the trace element content and internal structure of quartz crystals from the central Swiss Alps [60] describes crystals with lamellae concentrated in the outer parts of the crystal [61]. Crystals of quartz from alpine-type fissures in Austria are lamellae predominantly in external parts.

The macromosaic structure of quartz crystals has been described by Friedlaender [62] as composed of slightly tilted and radially arranged wedge-shaped sectors. They are recognized by the presence of sutures on the crystal faces, which are often confused with twin boundaries. Quartz with a macromosaic structure is typical for pegmatites, miarolitic pockets, and high-temperature alpine-type fissures. These crystals are sometimes called “Friedlaender quartz” or Macromosaic quartz.

Lamellar and macromosaic structures are responses of the crystal to disturbances during its growth and the resulting lattice defects. An ideally developed crystal does not manifest these types of internal structure defects.

Inclusions in quartz

Numerous textbooks and publications have dealt with mineral and fluid inclusions (FI) in quartz [63–68]. Fluid inclusions, either aqueous solutions or gases, sometimes arranged in regular planes, are common in quartz. For example, the color of milky quartz may be due to numerous minute fluid inclusions. Rock crystal, on the other hand, often has inclusions of rutile or schörl (black tourmaline). Quartz may contain inclusions of native gold, actinolite, goethite, hematite,

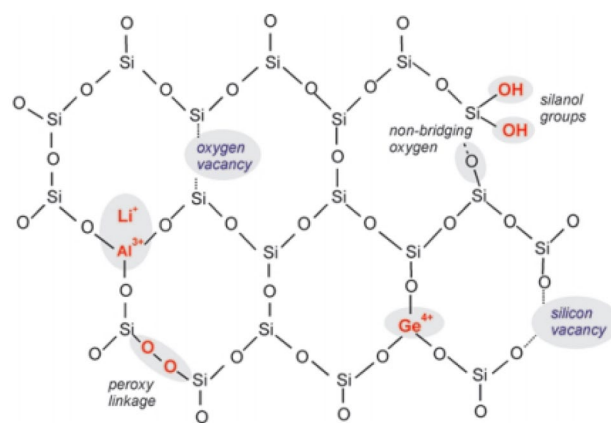


Fig. 11 Schematic quartz structure showing the most common defect types [14] (reprinted with permission from Cambridge University Press)

iron hydroxides, tourmaline, dumortierite, etc. The presence of fluid inclusions is one of the most important quality characteristics of natural quartz as a raw material, along with the contents of impurity elements and mineral inclusions.

Point defects in quartz

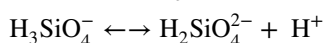
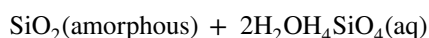
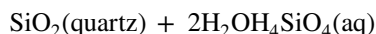
Point defects in quartz can be related to the incorporation of foreign ions of some chemical elements (e.g., Al, Ti, Ge, Fe, H, Ag, Cu, and P) at lattice and interstitial positions, to different types of displaced atoms, and/or to defects associated with Si or O vacancies. According to their characteristics, these defect centers are often classified as either intrinsic or extrinsic. Intrinsic point defects involve atoms of the host lattice only (missing atoms = vacancies, atoms at interstitial positions, and excess atoms), whereas extrinsic point defects belong to foreign atoms at lattice and interlattice positions [14]. To date, more than 20 different types of point defects in quartz have been determined [69–72]. The most common defect types in quartz are shown schematically in Fig. 11.

Solubility of SiO₂ in water

The aqueous chemistry of silica (SiO₂) is complex and involves coupled processes such as dissolution/precipitation, complexation to cations and anions in the aqueous phase, and complexation to cations and anions at the particle–water interface [73]. The dissolution of silica is strongly pH dependent in that silicic acid, Si(OH)₄ (the only form of silicon in soil waters that is available for entry or uptake into a plant), is formed at pH values ≤ 9–10 [73–75]. This conclusion results from its pK_a value of 9.6 [74], which means that it is a very weak acid and remains neutral under

almost all possible soil-water conditions [75] (it does not lose its first proton from any of the hydroxyl groups at pH below 10). The acidic properties of a silica surface have been described by an acidity constant for surface SiOH groups [74]. Silicic acid in natural waters polymerizes to form high-molecular-weight silicates [76] with two- and three-dimensional structures [77]. Three different processes for polymerization of silicic acid have been proposed to occur, via (i) monomer–monomer, (ii) monomer–polymer, and (iii) polymer–polymer interactions [78].

The solubility of silicon dioxide in water depends on temperature, pressure, its surface structure, and its structural modifications [22]. At temperatures above 100 °C and high pressures, the solubility of quartz increases rapidly. At 300 °C, depending on the pressure, it ranges between 700 and 1200 mg/l. SiO₂ dissolves poorly in water (although the solubility is higher for amorphous than crystalline silica) by forming orthosilicic acid, H₄SiO₄ (Si(OH)₄), which is a very weak acid. At low pH, the following reaction is sufficient to describe the solubility of silica in water:



The total dissolved silica concentration is $[\text{SiO}_2]_t = [\text{H}_4\text{SiO}_4] + [\text{H}_3\text{SiO}_4^-] + [\text{H}_2\text{SiO}_4^{2-}]$.

Figure 12 shows the solubility of quartz and amorphous silica (opal) with pH, as given by Karkanis et al. [79].

Color

Chemically pure quartz is colorless and transparent, but the presence of trace element impurities may result in a whole range of colors [80–84]. Natural quartz has four important colored varieties: citrine (yellow), amethyst (violet), smoky–morion (smoky to dark smoky), and prasiolite (green). Each of these varieties contains either a substitutional or interstitial component other than Si. Small amounts of trivalent Al and Fe and monovalent Na, Li, and K are frequently incorporated into quartz. Depending on the oxidation states and the site distributions of these foreign cations, these impurities may cause distinct coloration [85]. The color of amethyst and some types of citrine is derived from an iron presence [86].

Citrine is a variety of quartz that ranges from yellow–orange to orange–brown. When amethyst is heated over the range of 300–560 °C, it loses the violet color and may become brown, yellow, green, or colorless. These changes have been reviewed and investigated [87, 88]. Most of the

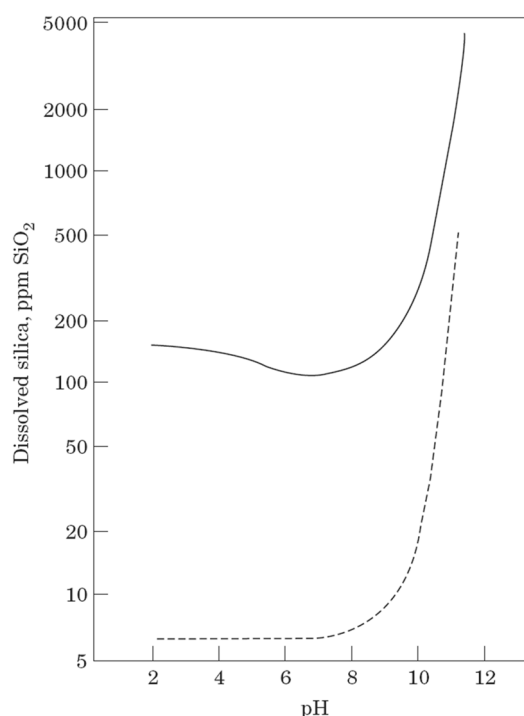


Fig. 12 Solubility of SiO₂ at 25 °C versus pH. The solid line is the solubility of amorphous silica (opal) as determined experimentally. The dashed line is the calculated solubility of quartz [79]. (Reprinted with permission from Elsevier)

citrine available today is produced by heat treatment of amethyst. Yellow coloration can also be produced by heating natural dark-brown or black smoky quartz to about 300 °C [89]. Green quartz, also called prasiolite or greened amethyst, is produced when amethyst is heated between 300 and 600 °C [87, 88]. Beautiful citrine crystals are presented in Fig. 13.

In thin sections, macrocrystalline quartz appears clear and homogeneous, with blue–gray to white or bright-yellow interference colors. Quartz grains do not show changes along the edges. Strained quartz grains from metamorphic rocks show a so-called undulatory extinction [91].

Other physical properties

Quartz shows practically no good cleavage, but there are literature reports on several directions of low cleavage: $\{10\bar{1}0\}$, $\{10\bar{1}1\}$, $\{01\bar{1}0\}$, $\{0001\}$, $\{11\bar{2}1\}$, and $\{11\bar{2}0\}$.

Fracture includes shells to half-shells in crystals, flat concave in massive aggregates, and uneven to hooked in fibrous aggregates.

Streaks may be colorless to white.

The luster is glassy to cloudy on crystal surfaces, or greasy to waxy on fractures.



Fig. 13 Citrine crystals from Olkhovka, Tyumenskaya Oblast, Polar Urals, Western Siberian Region, Russia [90] (with kind permission from Rob Lavinsky)

According to the Mohs hardness scale, quartz has a hardness of 7, whereas its absolute hardness is 100 [92, 93]

Its density is 2.6–2.7 g/cm³.

Optically, it is transparent, colorless and lies in optical class uniaxial (+).

The refractive index is $n_{\omega} = 1.543\text{--}1.545$ and $n_{\epsilon} = 1.552\text{--}1.554$.

The birefringence is +0.0090.

Quartz crystals exhibit piezoelectric properties (developing an electric potential under the action of mechanical stress) [94].

These physical properties of quartz were taken from Refs. [95–98].

Varieties of quartz

The different varieties of quartz are usually classified into two groups [17]: **macrocrystalline**, and **crypto-** or **microcrystalline**.

Macrocrystalline varieties are those that form crystals, such as amethyst, or have a macroscopical crystalline structure [99]. When people talk about “quartz,” they usually think of macrocrystalline quartz. The most common macrocrystalline forms are briefly described below.



Fig. 14 Rock crystal from Budinarci, RN Macedonia (photo R. Jankuloski)

Rock crystal

This name is given to all clear, colorless quartz crystals. Rock crystal can be artificially turned into smoky quartz by exposure to high-energy radiation. Rock crystal is found in any geological environment that allows quartz formation in general. Large, well-formed and transparent crystals are registered in some pegmatites, alpinotype vugs, and hydrothermal veins. Rock crystal often has inclusions of other minerals, which sometimes produce popular varieties of ornamental stone. Golden rutile inclusions produce a unique stone aptly named “rutilated quartz” that has a very hair-like look. Another variety is called “tourmalinated quartz” and contains intricately crossing needles of schörl (black tourmaline) trapped in the clear crystal [100, 101]. Marvelous samples of rock crystal are known to exist in RN Macedonia [102], one of which is presented in Fig. 14.

Smoky quartz

This is a smoky-gray, brown to black variety of quartz. Its color results from gamma irradiation and the presence of traces of aluminum built into its crystal lattice [103, 104]. The irradiation causes Al³⁺ atoms (that replace Si⁴⁺ in the lattice) to transfer an electron to a neighboring monovalent cation (often Li⁺) that is inserted in the lattice to charge compensate the replacement of Al³⁺ with Si⁴⁺. Smoky quartz can also be synthesized in the laboratory by irradiation of colorless quartz with gamma rays, which produces defects. The topic of aluminum centers in quartz has been a subject of interest in literature [104–108]. A beautiful sample of smoky quartz is presented in Fig. 15.

Amethyst

This is a violet to purple variety of α -quartz. The color of amethyst develops in the presence of traces of iron built into its crystal lattice [109], i.e., traces of Fe³⁺ as an initial



Fig. 15 Smoky quartz from Alinci, North Macedonia (photo R. Jankuloski)



Fig. 16 A cluster of large amethyst crystals from Rio Grande do Sul, Brazil (photo P. Makreski)

impurity that substitutes Si^{4+} in the α -quartz structure [110], with charge neutralization usually achieved by an alkali-metal ion placed on the twofold axis of the center. The Fe^{3+} site, after irradiation, is changed into Fe^{4+} , which is an uncommon valence state of iron [111]. The characteristic deep-blue transmission occurs from absorption due to $\text{O}^{2+} \rightarrow \text{Fe}^{4+}$ charge transfer, centered in the yellow–green region [110]. The amethyst color is destroyed by heat, but may be restored by ionizing radiation if the heating is not excessive. Figure 16 depicts splendid crystals of amethyst from Rio Grande do Sul, Brazil [112].

Aventurine

This variety of quartz contains glistening fragments (usually mica, such as fuchsite) that deliver its most common green

color, but it might also contain hematite (orange) or goethite (brown).

Ametrine

Ametrine crystals are made of alternating sectors of purple and yellow to orange color. Slabs cut perpendicular to the c -axis of the crystal provide a form that resembles a pinwheel.

Blue quartz

The color of natural blue quartz is due to scattering of incident light by minute inclusions [113]. This can be convincingly demonstrated by holding a thin slab of blue quartz such that light can reflect off the surface. Under these conditions, the blue color is observed. When the same slab is held such that it can be observed in transmitted light, the blue color is replaced by an orangish-brown color. According to Van Vultee and Lietz [114], the color of blue quartz is the result of Rayleigh scattering from inclusions of rutile needles, whereas Zolensky et al. [115] ascribe the origin of the blue coloration of quartz to the presence of fluid inclusions, apatite and zircon, fibrous magnesioriebeckite, crocidolite, or tourmaline.

Citrine

Citrine is a variety of quartz with color ranging from yellow to orange or orange–brown, according to early research, due to ferric impurities. Bukanov and Markova [116] observed that the citrine color occurred naturally in quartz crystal deposits in the USSR with high Li contents ($> 10^{-4}\%$ Li). According to Aines and Rossman [117], Bolivian and Indian quartz crystals with both amethyst and citrine zones have molecular water in the citrine zones and dominantly hydroxide ions in the amethyst zones. Citrine colors can occur in naturally irradiated quartz or can be produced by artificial irradiation of natural quartz from certain localities, by heat treatment of natural smoky quartz, or by heating quartz turned to smoky through laboratory irradiation. After quartz is subjected to extended electrolysis in water vapor and then exposed to ionizing radiation, citrine color centers are produced [118]. Greenish-colored dyes produced by the irradiation of natural and synthetic quartz with gamma rays are also described in literature [119–121].

Ferruginous quartz

This variety of quartz is colored red, brown, or yellow by inclusions of hematite or limonite.



Fig. 17 Rose quartz from Itinga, Minas Gerais, Brazil [130] (with kind permission from fabreminerals.com, photo and specimen)

Milky quartz

This is a semitransparent to opaque white-colored variety of quartz. The color may be due to the introduction of numerous minute fluid inclusions of gas, liquid, or both during the process of crystal formation [122].

Rose quartz

The color of rose quartz originates from fibrous inclusions of a pink borosilicate mineral related to dumortierite (aluminum borosilicate: $\text{Al}_{6,5-7}[(\text{O},\text{OH})_3(\text{BO}_3)(\text{SiO}_4)_3]$) [123–125]. Depending on the Fe and Ti content in the fibers, their color ranges from rose to colorless or blue. The presence of titanium color centers in rose quartz has been studied by Wright et al. [126]. The color of the fibrous mineral as well as the color of rose quartz is stable up to temperatures of about 575 °C [125, 127] and is also generally stable under ultraviolet light [125], although there have been occasional reports of materials that pale quickly in daylight. Rose quartz from some localities shows asterism when cut in the form of spheres or cabochons, much like that seen in certain sapphires. This is sometimes called star rose quartz. The six-rayed star is caused by reflections of light from embedded fibers that intersect at an angle of 60°. The position of the star depends on both the location of the light source and the position of the observer [128, 129]. A crystal aggregate of rose quartz is shown in Fig. 17.

Green quartz

Brazilian green quartz was described by Nassau and Prescott [121], while rare varieties of green quartz crystals from

quartz-agate geodes from Poland are described by Platonov et al. [131]. Natural occurrence of green quartz is rare.

Prasiolite

This is a transparent green variety of macrocrystalline quartz. It is a rare mineral in Nature. Most prasiolite is produced artificially by heating amethyst, being therefore sometimes called green amethyst, amegreen, or vermarine [132].

Tiger's eye

This mineral contains fibers of crocidolite (fibrous forms of riebeckite $\text{Na}_2(\text{Fe}_3^{2+}\text{Fe}_2^{3+})\text{Si}_8\text{O}_{22}(\text{OH})_2$) altered to a yellow color, also being known as “falcon's eye.” It is a less common variety.

Cat's eye

This is a black to grey stone with a silver–white streak.

Hawk's eye

This opaque blue stone is made of microcrystalline quartz.

Herkimer diamond

The term “Herkimer diamond” is a collective name for transparent (very clean), lustrous rock crystal quartz that forms attractive, regular hexagonal–bipyramidal crystals [133]. These crystals are formed under low-temperature hydrothermal conditions in sedimentary rocks and are often accompanied by inclusions of petroleum or associated with oil or coal deposits [133, 134]. The crystal exhibits very shiny surfaces, incredibly high clarity, short, stubby bodies, and double terminations and represents the only naturally double-terminated (a crystal with natural faces on both ends), water-clear, quartz crystal on Earth [135]. It is interesting that these beautiful gemstones appear already faceted and are very old. According to some estimates, these crystals are reported to be about half a billion years old [135].

“Herkimer diamond” is in fact a misleading name because the sample is not diamond. Apart from the confusion that the mineral is actually quartz rather than diamond, the name was established locally to describe quartz crystals found in the vicinity of Herkimer region, New York State, USA (since the early twentieth century and possibly even longer) [134]. Herkimer County, obviously, still remains the most famous source, but alternative names for this quartz have also emerged, including Middleville diamonds (named after the town of Middleville, New York, USA), Mohawk Valley

crystals (after a valley in Herkimer County, New York), and Little Falls diamonds (after the rock formation that hosts the mineralization) [136]. Despite these sites, the literature continuously cites other locations worldwide, in Tyrol (Austria), Tuscany (Italy), and Northern Cape (South Africa) [136], and recently in the Zagros Mountains, Kermanshah and Kurdistan Provinces (northwestern and northern Iran), where Herkimer-type quartz has been used in traditional jewellery for at least 100 years [133].

The hunt for Herkimer diamonds [137] resulted in the collection of crystals that differ vastly in size and range from several millimeters to much larger scale. Perfect crystals are usually less than ½ inch (1.27 cm) long, although much larger crystals are found occasionally [135]. Thus, although badly fractured and lacking the typical sparkling clearness, Francis [138] in 1953 reported a sample of 18 pounds (8.17 kg) measuring 10 inches (25.4 cm) from termination to termination, 24 inches (60.96 cm) in circumference, and with diameter of 7 and 8.5 inches (17.78 and 21.59 cm). The dimensions of this crystal were exceeded by the even larger Arkansas Herkimer diamond weighing 25 pounds 3 oz (11.42 kg) [139].

Although SiO₂ is the primary constituent of Herkimer diamonds, samples may occasionally contain inclusions of iron pyrite, air, water, or more commonly pieces of black fossilized organic plant material (black coal) formally called “anthraxolite” [135].

Cryptocrystalline or microcrystalline quartz comprises varieties that do not show any visible crystals and have a dense structure, like agate. Cryptocrystalline varieties are sometimes grouped together under the term “chalcedony.” A brief description of the most common crypto- or microcrystalline forms is given below.

Chalcedony

This is a more general term for all varieties of quartz that are built up of microscopic or submicroscopic crystals, i.e., the so-called microcrystalline varieties of quartz [140]. Chalcedony is a white, buff, or light tan, finely crystallized or fibrous quartz that forms rounded crusts, rinds, or stalactites (mineral deposits suspended from the roofs of caverns) in volcanic and sedimentary rocks as a precipitate from moving solutions. Figure 18 shows beautiful sample of chalcedony from Arizona, USA.

Agate

Agate is a distinctly banded fibrous chalcedony originally reported from Dirillo River (Achates River), Acate, Ragusa Province, Sicily, Italy. It appears as colorless, gray, red,



Fig. 18 Chalcedony from the Miami Mining District, Arizona, USA [141] (with kind permission from Rob Lavinsky)



Fig. 19 Agate from South Dakota, USA [143] (credit: James St. John, <https://creativecommons.org/licenses/by/2.0/>)

white, or any color due to embedded minerals, including multicolored specimens, which are very common. Some agates have reddish bands from iron oxide, while others from some localities in south Brazil are often nearly devoid of color in their natural state [142]. A wonderful sample of agate is shown in Fig. 19.

Carnelian

This is a reddish variety of chalcedony.

Chrysoprase

Chrysoprase is the name for a translucent variety of chalcedony that ranges in color from yellow–green to a more apple green. Chrysoprase stones result from lateritization or deep weathering of nickeliferous serpentinites and other ultramafic ophiolite rocks. It usually has a fibrous structure but may also be microgranular. According to Barasanov and Yakovleva [144] and to Heflik et al. [145], the color appears from finely distributed bunsenite (NiO). On the other hand, according to Faust [146] and Sachanbinski et al. [147], the color is due to finely disseminated hydrous nickel silicates

such as garnierite and saponites. These minerals are usually associated with chrysoprase deposits.

Sard

This is a brown to brownish-red translucent variety of chalcedony.

Onyx

In correct usage, the name refers to a (usually) black and white banded variety of agate, or sometimes a monochromatic agate with dark and light parallel bands.

Plasma

Plasma is a microgranular or microfibrinous variety of quartz showing colored variation with green shades arising from the disseminated particles of silicates such as chlorite, amphibole, celadonite, etc. It is opaque with conchoidal to smooth fracture [148].

Jasper

Geologically, the name has long been used for an opaque to slightly translucent, generally red or brown to variably colored, impure chalcedony or microcrystalline chert, usually containing abundant fine inclusions of hematite, iron hydroxides, and other minerals. Jasper is a massive, fine-grained quartz with relatively large amounts of admixed material, chiefly iron oxide, up to 20% or more [149]. It can also be brown, brownish yellow or ocher yellow, less commonly grayish green.

Chert

Chert is a very fine-grained quartz, a silica mineral with minor impurities. Several varieties are included under the general term chert, including jasper, chalcedony, agate, flint, porcelanite, and novaculite. Colors range from gray–black, gray–pale yellowish, reddish brown, to nearly white and arise from the same components found in jasper.

Flint

In prehistory, flint was a widely used raw material [150]. It is gray to black and nearly opaque (translucent brown in thin splinters) because it contains carbonaceous matter. Flint was used during the Stone Age for making tools, such as knives, and even until the nineteenth century to produce sparks by hitting steel for ignition of easily ignitable organic material. There are only a few reports of flint mining sites in the early Paleolithic, such as the Acheulian complex at Isampur, India



Fig. 20 Cristobalite from Auvergne, France [159] (credit: Eveline de Bruin from Pixabay)

[151], the Lower–Middle Paleolithic in Mount Pua (Israel) [152], and the Middle Paleolithic in Qena (Egypt) [153]. A number of flint sources in Bulgaria are well known and have previously been described in the archeological and geological literature [154–156]. Olofsson and Rodushkin have published a pilot study involving Scandinavian flint [157].

Heliotrope

This is an opaque green jasper with red spots of hematite or red jasper resembling spots of blood. Heliotrope is also called bloodstone [158].

Cristobalite

Named after the locality of Cerro San Cristobal, Mexico, cristobalite is a stable form of silica (silicon dioxide, SiO_2) between its melting point of 1728 °C and 1470 °C, below which tridymite is a stable form. Cristobalite has two modifications: low cristobalite, which occurs naturally up to 268 °C but is not stable, and high cristobalite, which occurs above 268 °C but is only stable above 1470 °C. Cristobalite has the same chemical composition as quartz, tridymite, stishovite, and coesite but a different crystal structure. Crystals of cristobalite are presented in Fig. 20.

High cristobalite (β -cristobalite) is cubic in space group $Fd\bar{3}m$ [117], while the low-temperature (α -cristobalite) form is tetragonal in space group $P4_12_12$ or $P4_32_12$ [160]. The unit cell parameters (α -polytype) are $a=4.9709(1)$ Å, $c=6.9278(2)$ Å, $V=171.18$ Å³, and $Z=4$. The transition from the α -form to the β -form results in a 4% increase in volume [161]. Cristobalite appears in the form of colorless, white, brown, grey, blue–grey, and yellow crystals. The luster is vitreous to subvitreous. Twinning is seen on {111}. Its hardness is 6–7, while the density is 2.32–2.36 g/cm³.

Cristobalite is transparent and very weakly birefringent. The optical properties are uniaxial (–). The refractive index



Fig. 21 Tridymite aggregate from Ochtendung, Eifel, Germany [163] (credit: Fred Kruijen, <https://creativecommons.org/licenses/by-sa/3.0/nl/deed.en>)

is $n_{\omega} = 1.487$ and $n_{\epsilon} = 1.484$. It possesses characteristic curving fracture lines.

Tridymite

This name comes from the Greek “*tridymos*,” meaning “triplet,” which alludes to its common twinning as trillings. Tridymite occurs in as many as seven polytypes, the most common at standard atmospheric pressure being known as the α - and β -forms. Below 100 °C, the triclinic form (α -tridymite) is stable. There are also orthorhombic, monoclinic, and hexagonal polytypes that are stable at higher temperatures. The orthorhombic polytype (β -tridymite) is most stable at elevated temperatures above 870 °C but converts to β -cristobalite above 1470 °C [162].

Tridymite is colorless, white, yellowish white, and gray. The cleavage on tridymite is indistinct $\{0001\}$ and imperfect $\{11\bar{1}0\}$. Its hardness is 6½–7 on the Mohs scale, while the density is 2.28–2.33 g/cm³. It exhibits very brittle fracture, producing small conchoidal fragments. Twins are common on $\{110\}$. Its optical properties are biaxial (+) with refractive index of $n_{\alpha} = 1.468$ –1.482, $n_{\beta} = 1.470$ –1.484, and $n_{\gamma} = 1.474$ –1.486; $2V(\text{measured}) = 40$ –86°. Tridymite is transparent, colorless to white, and in transmitted light is colorless. Tridymite usually appears in association with cristobalite, sanidine, quartz, augite, fayalite, hematite, ferroan, enstatite, and troilite. Figure 21 shows crystals of tridymite.

The most stable form of low tridymite, known as α -tridymite (under 100 °C), crystallizes in the triclinic system with unit cell parameters of $a = 9.932(5)$ Å, $b = 17.216(6)$ Å, $c = 81.854(9)$ Å, $\alpha = 90^{\circ}$, $\beta = 90^{\circ}$, $\gamma = 90^{\circ}$,

and $V = 13,996.16$ Å³ (calculated from the unit cell), with $Z = 320$ [164].

In 2010, Podwórny and Zawada [165] published the results of the refinement of the crystal structure of low-temperature tridymite in refractory silica materials. They found that α -tridymite occurs in two coexisting forms crystallizing in monoclinic space groups $C1$ and $F1$.

Coesite and stishovite

The high-pressure polymorphs of SiO₂ are coesite, belonging to crystal class 2/m and stishovite in crystal class 4/m 2/m 2/m. They are formed by shock metamorphism associated with the impact of giant meteorites.

Opal, SiO₂·nH₂O

The origin of this name is uncertain. It is most probably related to the Sanskrit word “*upala*,” meaning “stone” or “precious stone.” Opal is a hydrated amorphous form of silica with water content ranging from 3% to 21% by weight, but most frequently between 6% and 10%. In contrast to the crystalline forms of silica, which are classified as minerals, due to its amorphous character, opal is classed as a mineraloid [166].

Opal is classified into four types: opal-CT, which contains cristobalite–tridymite; opal-C, which contains cristobalite; opal-AG, which is amorphous (amorphous–gel) with closely packed amorphous silica spheres that form a diffraction grating to create precious opal; opal-AN, which is amorphous (amorphous–network) and found as hyalite. Transitions between opal-AG, opal-CT, and opal-C are common.

Opal appears in many color varieties because of the presence of impurities (color centers) that give it its white, yellow, red, blue, green, orange, brown, or black color. However, the color of some opals is partly due to light scattering, diffraction, and interference caused by the microspheres. Thus, the mineral exhibits an interesting diversity of colors and self-assembling color interplay that is found in Nature (butterfly scales, bird feathers, plants, insects) [167].

In precious opal, a rich play of colors or “fire” arises owing to the diffraction of white light by the spaces between tiny, uniformly sized silica spheres that are three-dimensionally regularly arranged [168]. Depending on the diameter of the silica spheres and the angle of the incident white light, one particular wavelength (color) is reinforced while the others are diminished by constructive and destructive interference, respectively. The spheres in the structure must exhibit a uniform diameter between 200 and 350 nm to be



Fig. 22 Opal from Česinovo locality, North Macedonia [170] (photo R. Jankuloski)

able to produce this play-of-color in the visible-light range from violet to red (400–700 nm). If the size of the spheres is too small (< 200 nm), the diffraction is insufficient to produce a visible play-of-color. In this case, the longest wavelengths that are reinforced are part of the UV light range and therefore invisible to the naked eye [168]. Also, such a play-of-color does not occur if the spheres are too large (> 350 nm) since the reinforced waves are located in the infrared range. However, if the stone is tilted, the wavelength that is reinforced becomes shorter and may move into the visible part of the spectrum so that (at first) red colors may start to appear. If the play-of-color exhibits three or more different colors, the main color followed by the term “multicolour” may be used.

Occasionally, the spaces between the submicroscopic silica spheres in opals may contain water or water-rich silica. Tyndall scattering at these inhomogeneities leads to bluish color in reflected light, while in transmitted light it looks yellowish [169].

Common opal does not exhibit a play-of-color because the silica spheres are not uniformly sized or not arranged in an orderly pattern, or because the spaces between the spheres are completely filled with silica [168]. An opal sample is presented in Fig. 22.

Its hardness ranges from 5½ to 6½ on the Mohs scale, whereas the density varies from 2.0 to 2.2 g/cm³. Opal fracture is conchoidal, while the luster is waxy or resinous. It appears in amorphous fragments or botryoidal forms, being transparent or translucent. Opal is isotropic ($n_{\alpha} = 1.40\text{--}1.46$, varying with water content), but may show birefringence due to strain.

Occurrence of quartz and its polymorphic modifications

Quartz is a common constituent of many igneous, sedimentary, and metamorphic rocks. It occurs in hydrothermal veins and pegmatites [171].

Pegmatite crystal deposits of quartz appear in many places in the world, but they are economically undervalued due to insufficient quality or small reserves of high-quality crystals. Quartz crystals are especially found in the middle parts of pegmatite bodies and can reach large sizes.

The greatest variety of shapes and colors of quartz crystals come from hydrothermal ore veins and deposits, reflecting the large differences in growth conditions (chemistry, temperature, and pressure) in these environments. The hydrothermal deposits of quartz crystals are formed mainly at intermediate temperatures. Spatially, quartz deposits are located in cracks in which the aggregates form nests, improperly located along the cracks. Quartz crystals are distributed along the walls of the cracks.

At higher temperatures and pressures, quartz is easily dissolved by watery fluids percolating the rock. When silica-rich solutions penetrate into cooler rocks, the silica will precipitate as quartz in fissures, forming thin white seams as well as large veins that may extend over many kilometers [149, 172, 173]. In most cases, the quartz in these veins will be massive, but they may also contain well-formed quartz crystals. Phyllites and schists often contain thin lenticular or regular veins of so-called segregation quartz [174] that run parallel to the bedding and are the result of local transport of silica during metamorphism [175]. Silica-rich fluids are also driven out of solidifying magma bodies. When these hot brines enter cooler rocks, the solution gets oversaturated in silica and quartz forms.

Euhedral quartz crystals that are embedded in igneous rocks are uncommon. Quartz is among the last formed minerals during the solidification of magma, and because crystals fill the residual space between the older crystals of other minerals, they are usually irregular. Euhedral, stubby bipyramidal quartz crystals are occasionally found in rhyolites. Only rarely are euhedral quartz crystals seen embedded in metamorphic rocks [176].

Alluvial–deluvial deposits of piezoptical quartz sometimes also contain economically interesting concentrations. Quartz crystals are nonevenly distributed in the sediments.

Cristobalite appears in sedimentary rocks [177]. Natural low-cristobalite usually occurs in sub-microcrystalline masses or fibrous to columnar spherulites in igneous rocks. It appears in cavities of volcanic rocks such as obsidian and rhyolite. Occurrence of metastable cristobalite in high-pressure garnet granulite has also been observed [178].

Tridymite appears in cavities and veins of trachyte and andesite lavas. It is deposited from hot gases in vesicles and

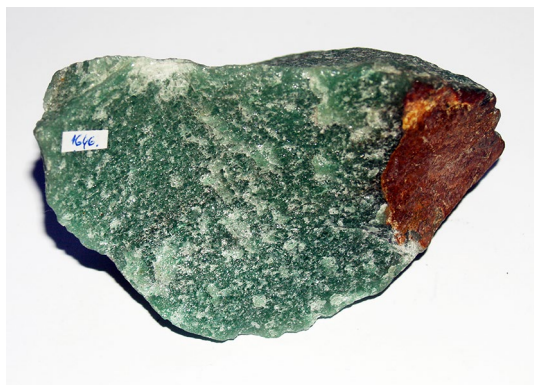


Fig. 23 Green quartz from Brazil (photo V. Bermanec)

lithophysae; as phenocrysts in felsic volcanic rocks, and less commonly, in basalts; in contact metamorphosed sandstone; also as the product of partial fusion of sandstone near igneous intrusions [179]. Tridymite deposits have been detected on Mars, but their nature and origin are uncertain [180].

Opal is formed by weathering and alteration of siliceous rocks and deposited in fissures, or as coatings and as replacements of fossils [181, 182].

Known localities of quartz in the world

Quartz appears in many places in the world, but the best known localities are found in Australia, Belgium, Brazil, Canada, China, Colombia, Egypt, Germany, Guatemala, India, Italy, Japan, Madagascar, Mexico, Namibia, Norway, Ukraine, Russia, Spain, Sri Lanka, Switzerland, Turkey, the USA, etc. [183, 184].

Fazenda Pacu in Brazil is one of the most productive areas in the world for large and pure quartz crystals [183]. Quartz crystals appear on a soft base of decomposed material. Of the hundreds of crystals unearthed, only one or two meet the requirements for piezopic quartz. The heaviest pure quartz crystal found at this site weighs a staggering 163 kg. Green quartz also appears in Brazil (Fig. 23).

Productive quartz deposits in Australia are located in northern New South Wales at the Kingsgate mining camp, 20 miles from Glen Innis [17, 185]. Guatemalan quartz deposits are located north of Guatemala City and occur in an area of gneisses and schists [186]. A productive quartz deposit has been developed in Colombia [187]. It consists of one principal vein and numerous subordinate veins. These veins are localized by fractures in a drag fold structure on the vertical limb of a tight anticline in the Cretaceous slates (Villeta Formation). Beautiful crystals of quartz from Boyacá Department, Colombia are shown in Fig. 24.



Fig. 24 Quartz crystals from Boyacá Department, Colombia [188] (credit: Géry Parent, <https://creativecommons.org/licenses/by-nd/2.0/>)



Fig. 25 Smoky quartz from Ural [189] (with kind permission from Rob Lavinsky)

In the Urals, there are numerous wires that contain economically interesting quartz crystals (Fig. 25) [189].

Crystal sizes of quartz are highly variable, from very small crystals up to extra large crystals (up to 200 cm long and 75–100 cm in diameter). In some deposits, which are characterized by significant sizes, crystals of quartz ores are oriented in the direction of inclination of the ore wires. One of the world's largest quartz clusters was discovered in 1985 in the Otjua mine near Karibib in Namibia at the bottom of a 45-m-deep cave (Fig. 26). It weighs 14,100 kg [190].

Fine specimens of quartz have been developed in many places in the Alps of Switzerland and Austria. Green to blue–green quartz is found in Rakowice Wielkie, Poland



Fig. 26 World's largest quartz crystal cluster (Museum in Namibia; size: 3 m wide, 3 m high; weight: 14,100 kg) [191] (credit: Mike W, <https://creativecommons.org/licenses/by-sa/2.0/>)



Fig. 27 Opal from Australia (photo V. Bermanec)

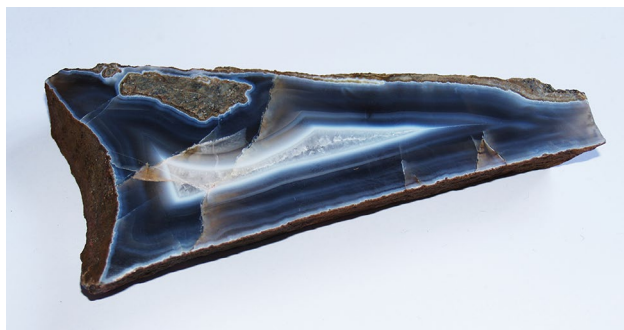


Fig. 28 Agate from Lepoglava, Croatia (photo V. Bermanec)



Fig. 29 Wood opal from Povraznik, Slovakia (photo T. Šíjaková-Ivanova)

[192]. A productive quartz deposit has been developed in Carrara, Tuscany, Italy [193].

Precious opal comes from Slovakia, Australia, and Mexico. Figure 27 shows blue opal from Australia.

Beautiful agates are found in Lepoglava, Croatia (Fig. 28). Wood opal from Slovakia is shown in Fig. 29.

Localities of quartz in North Macedonia

The evolution of the geological structure in the territory of North Macedonia allowed the formation of different types of silica raw materials. Quaternary continental formations are the most important bearers of secondary silicate materials such as quartzites and secondary quartz deposits [194, 195]. Four separate formations are the most notable bearers of these materials: moraine sediments, fluvial–glacial sediments, proluvial sediments, and alluvial sediments. Quartz deposits in North Macedonia vary in terms of their exploitation conditions and quality. Basically, primary deposits are characterized by especially high quality in relation to secondary deposits, but primary quartz deposits are limited in reserves and very difficult to exploit. On the other hand, secondary deposits of quartz contain larger reserves and offer conditions better suited for exploitation [196]. Regarding quality, they offer lower quality, excluding some localities where high-quality quartz samples emerge (Babuna, Plačkovica, Ogražden, and Selečka Planina).

Crystal quartz samples of significant quality are found around the Villages of Budinarci and Mitrašinci and also in the Pelagonian Massif [197, 198].

Pegmatite quartz deposits appear at the localities of Alinci and Belutče. They have an almost uniform monomineral composition of quartz crystals. Locally, pigmentations in the quartz mass appear with limonite in small cracks [199].

Deposits of wire quartz mainly appear in gneiss–micaschist formations or granite intrusions. In their composition, it is



Fig. 30 Quartz from Alinci (photo R. Jankuloski)

often possible to find lower contents of plagioclases, potassium feldspars, tourmaline, rutile, sericite, biotite, and kaolin. High-quality wire quartz is excavated at the localities of Orehovo, Umlenna, Preseka, Prevedena, and Ribnica and the mountains of Babuna, Plačkovica, and Ogražden [200].

The most important deposits of quartzite lie in the western and central part of North Macedonia: Skopska Crna Gora, and the Villages of Vozarci, Čičevo, Raven, Vrutok, and Ratkova skala [190].

Secondary quartzites have a quartz–chalcedony mineral composition. These deposits are found only in the Kratovo–Zletovo volcanic area (Crn Vrv, Plavica, and Pešter) [201, 202].

The largest and highest quality quartz sands are found in the Skopje tertiary basin in the vicinity of Dolno Sonje [196]. There are large deposits of quartz sand on both sides of the Markova Reka (River), near the Villages of Batinci and Varvara [196]. The largest quantities of and best-quality quartz sands are found in Dolno Sonje. These are chemically pure silicon dioxide with 99 wt.% SiO₂.

Alinci locality

The geology of the Alinci locality is characterized by alkali syenites, amphibolites, gneisses, and muscovite schists and marbles [203]. Quartz crystals emerge in aplite and pegmatite veins, which are basically built up of quartz and microcline [203]. Quartz crystals are filled with needles of arfvedsonite, which is a very common mineral at this locality. A quartz crystal from Alinci is shown in Fig. 30.



Fig. 31 Quartz from Čanište (photo R. Jankuloski)

Čanište locality

The Čanište locality lies on the western edge of Selečka Planina. The dominant part of the quartz at Čanište is massive. Beautiful quartz crystals appear in the gaps of the pegmatite body. The pegmatite body is lens-formed, but deep in the ground it becomes thinner and adopts a vein structure. It is mainly made from feldspars (amazonite), muscovite, garnet, biotite, and quartz [84]. A quartz crystal from Čanište is shown in Fig. 31.

Budinarci locality

Budinarci Village is situated about 12 km northeast of the Town of Berovo. The rocks around the village are composed of micashists, amphibolite, gneisses, and granites. Based on previous research [194, 197], piezoptic quartz crystals appear in three ways: in completely kaolinized granites, in granite cracks, and inside quartz wires themselves. Quartz veins, which generically have pegmatite origin, intercept the gneisses very irregularly. The size of the veins varies, and quartz appears as either well-formed crystal aggregates or beautiful monocrystal species, from transparent, through slightly smoky, to totally dull. The commonest form of quartz is completely kaolinized granites, being found over an area of about 1 km². The granite along the fault structures is completely kaolinized, and the quartz crystals occur in the form of arrays with ideally developed forms of the crystal system, or most often in the form of druse. Quartz in granite is quite rare, but still interesting as an occurrence. Quartz crystals are evidenced in the centers of the granite 10–20 cm open cracks. The development of the crystals is quite regular, and their base is always flat. The most common crystal forms are {10 $\bar{1}$ 1}, {11 $\bar{2}$ 1}, {10 $\bar{1}$ 0}. It rarely occurs as individual crystals, but they are usually buds of different sizes. Piezopic quartz crystals are also found in the quartz wires themselves. In granites, in the contact parts with the shales,



Fig. 32 Quartz from Budinarci (photo R. Jankuloski)



Fig. 33 Quartz from Belutče (photo R. Jankuloski)

there are quartz wires with quite small dimensions, 5–20 m long and 1–3 m thick. In these quartz wires, well-developed individual quartz crystals or quartz druses are found filling the hollow sections of quartz wires. Their appearance is quite uneven and unpredictable. A quartz crystal from Budinarci is shown in Fig. 32.

Belutče locality

The Belutče locality is situated in the southern part of Mariovo. Basically, it lies on a quartz pegmatite vein. The main minerals in this vein are quartz, orthoclase, microcline, and apatite [195]. Quartz crystals are ideally developed and reach 15 cm in length. As well as transparent quartz crystals, crystals of smoky quartz also appear at this locality. A quartz crystal from Belutče is shown in Fig. 33.



Fig. 34 Quartz from Sasa (photo R. Jankuloski)

Sasa ore field

The area comprising the Sasa ore field is made up of schistose mica granitoporphyrite, quartz diorite–plagiogranite, quartz latites, graphite, phyllite schists, cipolines, and scarns. The scarns occur in a series of quartz graphite schists and cipolines.

The mineral composition of the ore mineralization in this locality is very complex and basically represented by a variety of minerals formed in different mineralization stages (metamorphic, skarn, hydrothermal) [204, 205]. In the hydrothermal stage of formation of the Sasa locality, intensive silification represented by small-grained quartz aggregates appeared. The aggregate replaces the basic gneiss minerals. The appearance of considerable amounts of well-shaped crystalline quartz (Fig. 34) is characteristic, as well as the common association of this mineral with galena, sphalerite, and occasionally carbonate minerals.

Zletovo ore field

The Zletovo lead–zinc deposit, located in the east of the Kratovo–Zletovo volcanogenic complex, occupies the central parts of the Kratovo–Zletovo ore district or the southeastern parts of the Zletovo ore field. The Zletovo lead–zinc deposit was formed by hydrothermal activity intimately associated with tertiary volcanism along the active continental margin. The major rock types in the area are andesite, dacite, dacitic ignimbrite, and volcanic tuff. Quartz appears in almost all phases of the mineralization processes in the Zletovo ore locality. The association of quartz and chalcedony is basically present in low-temperature oxide carbonate paragenesis, where quartz appears accompanied with siderite, rhodochrosite, calcite, and barite [206, 207]. The formation of either crystal quartz aggregates or monocrystals in all the



Fig. 35 Quartz from Zletovo (photo R. Jankuloski)

mentioned different temperature stages is typical. In the quartz grains, fluid inclusions were identified and measured, being almost evenly distributed [68]. Quartz crystals from Zletovo are shown in Fig. 35.

Češinovo locality

In the Kratovo–Zletovo volcanic area, especially in the Češinovo locality, a great content of volcanic tuffs occurs [208, 209]. Opalization (Fig. 22) is a postvolcanic occurrence as a result of the influence of the hydrothermal solution (rich in silicium) on the tuffs. The most dominant part of the hydrothermal changes is represented by opal. Opalization processes are related to the Neogene volcanism on the territory of North Macedonia. They are the end-product of volcanic activity. The texture and different color varieties of opal occur as a consequence of the intensity of the process of hydrothermal metamorphosis on the tuffs. Some of them are characterized by the presence of tridymite on their surface [84].

Saždevo locality

A gneiss–micashists series appears in the contact part of the Pelagonian–Metamorphic Complex and the West-Macedonian Zone near Saždevo Village. Here, quartz lenses appear, occasionally reaching 10 m in length. These lenses are sometimes additionally followed by well-developed quartz crystals [210]. Complete chemical analysis revealed that the trace element content was the only reason for the different colors of these quartz samples. Thus, the red color of quartz and opal is connected with the presence of Fe, the green varieties have significant amounts of Ni, Ca leads to milky-colored samples, and light- or dark-brown to black color is due to the presence of Al, Pb, and Mn trace elements [84] (Fig. 36).



Fig. 36 Quartz from Saždevo (photo R. Jankuloski)

Diagnostic features of quartz

Quartz is easy to identify based on the combination of the following properties [211]:

- Crystal form (generally hexagonal prisms that terminate at each end with a six-sided pyramid, although the entire crystal may not be perfect, depending on the quartz formation process);
- Poor to indistinct cleavage;
- Hardness (easily scratches glass);
- Glass-like luster;
- Conchoidal fracture in crystals. In massive specimens, the fracture often looks irregular to the naked eye, but still conchoidal at high magnification. In macrocrystalline quartz, the fracture surfaces have a vitreous to resinous luster, whereas in cryptocrystalline quartz (chalcedony), fractured surfaces are dull.

Quartz may be confused with some calcite. It is distinguished from calcite by its high hardness.

Uses of quartz

Quartz is widely used as a raw material in several industrial applications [212]. Quartz sand is used in the production of glass, flat-plate glass, specialty glass, and fiberglass. Quartz is an excellent abrasive material. Quartz sands and finely ground silica sand are used for sand blasting, scouring cleansers, grinding media, and grit for sanding and sawing. Refractory bricks are often made of quartz sand because of its high heat resistance. It is also used as a filler in the

manufacture of rubber and paint. Quartz sands are used in the building industry for concrete and mortar.

Quartz sand is also used as a material for ferrosilicon and silicon production [213]. Some phonographs use quartz crystals to convert the vibrations of the stylus (needle) into electric impulses. For electronic use, a quartz crystal must be flawless [214]. Quartz and its varieties have been used since antiquity as semiprecious gems, ornamental stones, and collector's items. It is hard, durable, and usually accepts a brilliant polish. Popular varieties of quartz that are widely used as gems include amethyst, citrine, rose quartz, smoky quartz, morion, and aventurine.

Quartz crystals have been in regular use for many years to provide an accurate frequency for all radio transmitters, radio receivers, and computers (as the important silicon semiconductors).

The piezoelectric property of quartz leads to its use in oscillators and pressure gauges, for which highly perfect crystals are required, being grown artificially nowadays. In particular, in the year 1880, the young brothers Pierre Curie (1859–1906) and Jacques Curie (1855–1941) discovered the piezoelectric effect [215, 216]. They found that, when a mechanical stress is applied to a crystal or certain materials, a potential difference is induced across the crystal (material), being proportional to the applied stress. They demonstrated this effect using tourmaline, quartz, topaz, cane sugar, and Rochelle salt (sodium potassium tartarate tetrahydrate). The next year, Gabriel Lippmann (1845–1921) found that the inverse of this effect, called the inverse piezoelectric effect, also occurs [217]. The newly discovered effect was quickly dubbed piezoelectricity to distinguish it from other scientific phenomena such as contact electricity (friction-generated static electricity) and pyroelectricity (electricity generated from crystals by heating). The term “piezo” comes from the greek word “πιέζειν” (*piezein*), which means to press or squeeze, indicating that piezoelectricity is the occurrence of mechanical strain upon the application of an external electric field to such crystals.

The piezoelectric effect originates from the molecular dipoles within these materials. If there is any charge imbalance in the molecule, the molecule will have a dipole moment. These dipoles tend to have the same direction when next to each other, together forming regions that are referred to as domains. As most of the dipoles are oriented in the same direction in a domain, each will have a resulting dipole characteristic. Although each domain has its own dipole moment, the overall crystal is nonpolarized because the domains are randomly oriented. However, when an external mechanical stress is applied to such a piezocrystal, its crystalline structure is disturbed and the orientation of these domains is changed due to this force. As the orientation of the dipole domains is no longer entirely random, there will

be an uneven charge distribution between the two faces of the crystal piece. As a result, a potential difference will develop across the crystal, causing the piezoelectric effect. On the other hand, when a strong electric field is applied across a piece of such crystal, the domains orient themselves in the direction of the applied field. Due to this change in the orientation of the domains, a mechanical stress in the crystal will emerge, corresponding to the aforementioned inverse piezoelectric effect. A more detailed elaboration of the history and the importance of this effect is given in the great work of Katzir [218].

Piezoelectric crystals are now used in numerous ways [219, and references therein]:

- Frequency standards (quartz clocks and quartz watches), being at least one order of magnitude more accurate compared with mechanical clocks [220], employ a crystal oscillator made from a quartz crystal that uses a combination of both direct and inverse piezoelectricity to generate a regularly timed series of electrical pulses. The quartz crystal (like any elastic material) exhibits a precise natural frequency that can be used to stabilize the frequency of a periodic voltage applied to the crystal. The first quartz watch was unveiled by Japanese watchmaker Seiko as the Astron in 1969 [221]. Thereafter, quartz became the crystalline material most widely used in timekeeping technology for producing clocks, watches, and other time measuring devices. The same principle is used in some radio transmitters, receivers, and in computers, where it creates a clock pulse. These usually apply a frequency multiplier to reach gigahertz ranges.
- High-voltage and high-power sources (cigarette lighters, energy harvesters for soldiers' boots, and charge batteries),
- Sensors (piezoelectric microphones, piezoelectric pickups for acoustic electric guitars, piezoelectric microbalances used as very sensitive chemical and biological sensors, piezoelectric transducers, etc.),
- Actuators (loudspeakers, ultrasonic cleaning, piezoelectric motors, acoustooptic modulators, atomic force microscopes, and scanning tunneling microscopes that employ inverse piezoelectricity to keep the sensing needle close to the specimen, inkjet printers, high-performance common-rail diesel engines that use piezoelectric fuel injectors, X-ray shutters, etc.),
- Piezoelectric motors (ultrasonic motors used for autofocus in reflex cameras, inchworm motors for linear motion).
- Infertility treatment (in people with previous total fertilization failure, piezoelectric activation of oocytes together with intracytoplasmic sperm injection (ICSI) seems to improve fertilization outcomes).

- Surgery (piezosurgery is a minimally invasive technique that aims to cut a target tissue with little damage to neighboring tissues),
- Many other potential applications.

Industrial production of quartz crystals

The historical evolution of the industrial production of quartz crystals is very well elaborated in the work of Bottom [222], although this work reflects on the timeline of events in the USA. The decision to produce quartz on a large scale was made in 1939 to address the need for military transmitter–receiver components for use in aircraft communications systems, because quartz crystal units were used in both the transmitter and the receiver part. Starting from that historical turning point prior to World War II, industrial electronic-grade quartz crystal remained a demanded material whose supply is majorly achieved through manufacturing rather than mining activities. The development of the first quartz growth process for commercial use dates from 1956 [223]. Since then, the manufacturing process has been improved to meet the greater technical demands of frequency control components.

In the past, cultured quartz crystal was primarily produced using lascas as raw quartz feed material. Lascas is a non-electronic-grade quartz that is used as feedstock for growing cultured quartz crystal and for the production of fused quartz [224]. In addition to lascas, companies may also use cultured quartz crystal as feed material. This quartz has usually been rejected during the manufacturing process because of structural imperfections. During the past few years, Asia (Japan, China, and Russia) has emerged as a primary source for cultured quartz crystals, whose production is growing continuously. Electronic devices still account for most industrial use of quartz crystal, demanding cultured rather than natural crystals [224]. Electronic-grade quartz crystals are a primary material for the fabrication of frequency filters, frequency controls, and timers in electronic circuits. These parts are incorporated into a wide range of products, such as communications equipment, computers, and many consumer goods, such as electronic games and television receivers [224].

Quartz crystals are continuously and largely being substituted by silicon for frequency-control oscillators in electronic circuits. As well as silicon, other materials with higher piezoelectric coupling constants find use as replacements for quartz crystal, including aluminum orthophosphate, langsite, lithium niobate, and lithium tantalate [224]. Today, single-crystal cultured quartz is the material most widely used in frequency control, ranking second only to silicon in terms of the quantity of single-crystal material produced for all electronic applications [223].

Industrial growth of quartz crystals

The production of synthetic quartz aims to meet the industrial demand for quartz crystals (for use primarily in electronics). Although synthetic quartz is dominantly manufactured by hydrothermal synthesis, the development of this process can be considered historically in three rather distinct phases: (1) fundamental work based on the mineralogical genetic viewpoint (from the end of the nineteenth to the beginning of the twentieth century, in Italy), (2) industrial application (during WW2, in Germany and England), and (3) industrialization of quartz growth (after WW2, in England, the USA, and Russia) [225]. The pioneer of hydrothermal quartz synthesis was Giorgio Spezia (1842–1911) [226], who in 1909 initiated the growth of quartz crystals in an autoclave [227], only for scientific purposes. The autoclave [225, 228] contained an upper and a lower part. The temperature in the upper part was set and maintained at around 300 °C using city gas, while the bottom part was water-cooled. In this autoclave, nutrient quartz dissolved in a hydrothermal solution was transported by downward diffusion and deposited on the seeds. The growth rate of the quartz crystals was about 0.02 mm/day (about 10–20 times slower in comparison with the industrial growth rate achieved nowadays using thermal convection of solution). The next historical leap toward faster growth rates was introduced by Richard Nacken (1884–1071) [229] using the isothermal method in hydrothermal solution based on the difference of solubility between fused quartz as nutrient and crystalline quartz as seeds [230]. Improvements in synthetic quartz growth were delivered practically at the same time by the temperature gradient method (using crushed quartz as nutrient) introduced by Ernest Buehler (1913–1988) [231] in collaboration with Walker [232]. The method was later improved by Brown et al. [233]. Nowadays, modern facilities enable the production of large quartz crystals of meters in size with SiO₂ purity above 99.9999 wt%. This level of purity is not found in natural quartz crystals. More scientific protocols regarding quartz crystal growth are described in Refs. [234–244].

Hydrothermal quartz growth starts in specially designed thick vessels that operate at high pressure (> 100 MPa) and moderate temperatures (300–350 °C). The feed material, which is usually broken pieces of natural quartz, is placed in the bottom of the vessel, then a perforated baffle is placed above the quartz feeder. A water solution is introduced into the vessel, meaning that “mineralizer,” a little sodium hydroxide or sodium carbonate, is also added to the water [245]. The liquid fills the vessel to about the 85% level, then “seed crystals” (usually flat plates of transparent quartz) are immersed in the solution from the top. Then, the vessel is sealed to withstand high pressure, and the heating of the mixture starts. Although quartz is very insoluble in water at

lower temperatures, further heating induces extra pressure that eventually leads to the formation of a liquid–gas phase. At this pressure (around 140 MPa) and around 300 °C, all of the water is turned to a gas, but the quartz itself is only slightly soluble even at this temperature and pressure. Therefore, the mineralizer helps the quartz to form a more soluble sodium silicate. Another necessary step is to design the heating to enable a gradient of 40 °C between the temperatures at the bottom and top of the vessel. Thus, the lower quartz (feed) is more soluble than in the top seed area and the system is held in thermal equilibrium. Quartz fed from the bottom (hotter region) travels up to the top area and is deposited on the slightly cooler seed crystals. Therefore, the top seed crystals grow as the bottom feed quartz is consumed. When sufficient growth time has been allowed, the heating jacket is turned off, the pressure is released, the system is opened, and the hydrothermally formed crystals are removed [245].

For more details regarding the hydrothermal process, the reader is invited to refer to Refs. [246–249].

Production of fused silica and its various applications

Silicon dioxide also exists as a noncrystalline form (glass) known as fused silica. Unlike borosilicate glass, this material has no additives and exists as pure SiO₂. The material can be produced in sheets and plates and is known as fused silica wafers [250]. It lacks a defined structure and long-range order because of its highly cross-linked three-dimensional atomic features. The fabricated material exhibits high purity, high transmission, and high refractive index homogeneity [250]. The volume of fused silica increases little because of its low thermal expansion coefficient, and it can withstand high temperatures. These characteristics explain its wide use in semiconductor, medical science, communications, lasers, infrared, electronics, measuring instruments, military, aerospace, and other high-technology industries [250].

Fused quartz is produced by melting (fusing) high-purity silica sand. Depending on the starting conditions and initial compounds, the production is restricted to four basic types of commercial products (type I–IV) [251]. For production of type I, natural quartz is melted by induction in a vacuum or in an inert atmosphere. Quartz Crystal powder is the starting reactant for type II fused quartz, being subjected to a high-temperature flame. The other two types (III and IV) are produced by burning SiCl₄ in a hydrogen–oxygen flame or in a water vapor-free plasma flame, respectively [252].

Fused quartz is the most important material in the telecommunications industry for production of optical fibers because of its wide transparency range, from the UV to mid-IR [251]. Another useful feature of this material for applications stems from its physical strength, enabling its use to construct the windows of telescopes, lenses, as well as the

windows of modular spacecraft or space stations (including the Space Shuttle and the International Space Station) [253]. Fused quartz is also a material widely applied to address the most demanding requirements of the semiconductor industry (substrates for projection masks for photolithography, substrates for high-precision microwave circuits), chip industry (windows on erasable programmable read-only memory), data storage (for 5D optical data), and other uses [251].

Conclusions

As a very abundant mineral, quartz is one of the most useful natural materials in the world. Its usefulness can be linked to its unique physical properties, which are related to its chemical composition and structure. Quartz can be found in many different geological environments, and its visual appearance reflects the various conditions during its formation. Quartz occurs in a great number of varieties that differ in form and color. It occurs as massive aggregates, dense nodules, or crystals in druses.

The silica minerals with the SiO₂ composition include many polymorphs, with quartz being the most common member, occurring in both a trigonal low-temperature form known as α -quartz and a hexagonal high-temperature form known as β -quartz. Other important silica polymorphs are α - and β -tridymite, α - and β -cristobalite, coesite, and stishovite. Opal is a solid silica gel containing a large amount of water.

Chemically pure quartz is colorless and transparent, but the presence of trace element impurities may result in a whole range of colors. Natural quartz has four important colored varieties: citrine (yellow), amethyst (violet), smoky–morion (smoky to dark smoky), and prasiolite (green).

The different forms of quartz are usually classified into two groups: macrocrystalline and crypto- or microcrystalline varieties.

Macrocrystalline varieties are those that form crystals or have a macroscopic crystalline structure. The most well known among these are rock crystal, smoky quartz, amethyst, citrine, milky quartz, aventurine, rose quartz, blue quartz, green quartz, prasiolite, and ametrine. Crypto- or microcrystalline varieties do not show any visible crystals, sometimes being grouped together under the term “chalcedony.” The members of this group are chalcedony, agate, carnelian, chrysoprase, sard, onyx, plasma, jasper, chert, flint, and heliotrope.

Quartz appears in many places in the world, with the most well-known localities being in Australia, Belgium, Brazil, Canada, China, Colombia, Egypt, Germany, Guatemala, India, Italy, Japan, Madagascar, Mexico, Namibia, Norway, Ukraine, Russia, Spain, Sri Lanka, Turkey, the USA, etc.

Quartz is widely used as a raw material in several industrial applications, including the production of various types of glasses, refractory bricks, as an abrasive material, as a filler in the manufacture of rubber and paint, in the building industry in concrete and mortar, as a flux in the smelting of metals, in the production of ferrosilicon and silicon metal ((Fe)Si), in electronic application, for providing an accurate frequency for all radio transmitters, radio receivers, and computers (as the important silicon semiconductors), as semiprecious gems, ornamental stones, and collector's items, as gems including amethyst, citrine, rose quartz, smoky quartz, morion, and aventurine, and in the production of quartz clocks and watches, which are at least one order of magnitude more accurate compared with mechanical clocks.

According to the mineral–petrographic characteristics in North Macedonia, the following types of quartz can be distinguished: pegmatite quartz, wired quartz, quartzite, and secondary quartzites.

In the territory of North Macedonia, significant deposits of crystalline quartz are known around the Villages of Mitrašinci and Budinarci and the Towns of Prilep and Bitola. Also, a number of deposits of high-quality quartz veins are known around Orehovo, Plačkovica, and Ogražden. In almost all tertiary basins, deposits of quartz sand can be found (at Dolno Sonje, on both sides of the Markova Reka, and the Villages of Batinci and Varvara). Large quartzite deposits can be found in many places such as Ratkova Skala and Crni Vrv and the Villages of Čičevo, Raven, and Vrutok. In addition to quartzites, there are a number of other raw materials in which silicon dioxide predominates, such as opalescent breccia and opalescent tuffs around the Towns of Kočani and Kumanovo. The largest quantities and best-quality quartz sands are found in Dolno Sonje. This is chemically pure silicon dioxide with 99% SiO₂.

Some of these localities are in the phase of being explored. Detailed investigations are required to determine their quality and their potential for use.

Funding This research was supported by Macedonian Academy of Sciences and Arts (grant 07-361/1).

References

- <https://mrdata.usgs.gov/major-deposits/map-us.html> (Accessed 21 Jan 2022)
- Theophrastus, History of stones. Edited and translated by Sir John Hill. London, 2nd edition, 1774
- Tomkief SI (1942) On the origin of the name quartz. *Miner Mag* 26:172–178
- Agricola G (1530) Quarzum. in: *Georgii Agricolae Medici Bermannus, Sive De Re Metallica*, in aedibus Frobenianis Basileae 88, 129
- Brown E (1685) *Travels in divers parts of Europe... with some observations on the gold, silver, copper, quick silver mines*. London, 2nd edition, p.170
- Henckel JF (1725) *Pyritologia oder Kiess-Historie*. Leipzig. English translation: *Pyritologia; or, a history of the pyrites, &c.* London, 1757
- <https://en.wikipedia.org/wiki/Quartz> (Accessed 21 Jan 2022)
- <https://de.wikipedia.org/wiki/Quarz> (Accessed 21 Jan 2022)
- <http://webmineral.com/danaclass.shtml#.YU7gHrgzaUK> (Accessed 21 Jan 2022)
- <http://www.webmineral.com/strunz.shtml#.YU7g8LgzaUK> (Accessed 21 Jan 2022)
- <https://www.mindat.org/cim.php> (Accessed 21 Jan 2022)
- Weil JA (1984) A review of electron spin spectroscopy and its application to the study of paramagnetic defects in crystalline quartz. *Phys Chem Miner* 10:149–165
- Weil JA (1993) A review of the EPR spectroscopy of the point defects in α -quartz: the decade 1982–1992. In: Helms CR, Deal BE (eds) *Physics and Chemistry of SiO₂ and the Si-SiO₂ interface 2*. Plenum Press, New York, pp 131–144
- Götze J (2009) Chemistry, textures and physical properties of quartz—geological interpretation and technical application. *Miner Mag* 73:645–671
- <https://serc.carleton.edu/details/images/32743.html> (Accessed 21 Jan 2022)
- Graetsch HA, Miede G (1992) Crystal structure of moganite: a new structure type for silica. *Eur J Miner* 4:693–706
- <https://www.mindat.org/min-3337.html> (Accessed 21 Jan 2022)
- http://www.quartzpage.de/gro_text.html (Accessed 21 Jan 2022)
- http://www.quartzpage.de/crs_intro.html (Accessed 21 Jan 2022)
- Hosaka M, Miyata T, Sunagawa I (1995) Growth and morphology of quartz crystals synthesized above the transition temperature. *J Cryst Growth* 152:300–306
- Rykart R (1984) Authigene Quarz-kristalle. *Lapis Mineralien Magazin*: 9(6)
- Rykart R (1995) *Quarz- Monographie*. Ott-Verlag – German Edition
- <https://www.mindat.org/photo-753794.html> (Accessed 21 Jan 2022)
- Lang AR (1965) Mapping Dauphiné and Brazil twins in quartz by X-ray topography. *Appl Phys Lett* 7:168–170
- McLaren AC, Phakey PP (1969) Diffraction contrast from Dauphiné twin boundaries in quartz. *Phys Status Solidi* 31:723–737
- Leydolt F (1855) Über eine neue Methode, die Structur und Zusammensetzung der Krystalle zu untersuchen, mit besonderer Berücksichtigung der Varietäten des rhomboedrischen Quarzes. *Sitzungsberichte der mathematisch naturwissenschaftlichen Classe der kaiserlichen Akademie der Wissenschaften* 15:59–81
- Van Goethem L, Van Landuyt J, Amelinckx S (1977) The α - β transition in amethyst quartz as studied by electron microscopy and diffraction. The interaction of Dauphiné with Brazil twins. *Phys Status Solidi* 41:129–137
- Weiss CS (1829) Über die herzförmig genannten Zwillingkrystalle von Kalkspath, und gewisse analoge von Quarz. *Abhandlungen der Königlichen Akademie der Wissenschaften zu Berlin* 77–87
- Sunagawa I, Yasuda T (1983) Apparent re-entrant corner effect upon the morphologies of twinned crystals; a case study of quartz twinned according to Japanese twin law. *J Cryst Growth* 65:43–49
- <https://opengeology.org/Mineralogy/6-igneous-rocks-and-silicate-minerals/> (Accessed 21 Jan 2022)
- http://www.quartzpage.de/px/rc_br_joaquim_felicio_Q271_1_org.jpg (Accessed 21 Jan 2022)

32. http://www.quartzpage.de/crs_twins.html (Accessed 21 Jan 2022)
33. <https://www.mindat.org/photo-266098.html> (Accessed 21 Jan 2022)
34. Antao SM, Hassan I, Wang J, Lee PL, Toby BH (2008) State-of-the-art high-resolution powder X-Ray diffraction (HRPXRD) illustrated with Rietveld structure refinement of quartz, sodalite, tremolite, and meionite. *Can Mineral* 46:1501–1509
35. Kihara K (1990) An X-ray study of the temperature dependence of the quartz structure. *Eur J Mineral* 2:63–77
36. Heaney PJ, Veblen DR (1991) Observations of the alpha-beta phase transition in quartz: a review of imaging and diffraction studies and some new results. *Am Miner* 76:1018–1032
37. Drees L, Wilding L, Smeck N, Senyaki A (1989) Silica in soils: quartz and disordered silica polymorphs. In: Dixon JP (ed) *Minerals in soil environments*. Soil Science Society of America, Madison, pp 913–975
38. http://www.quartzpage.de/gen_struct.html (Accessed 21 Jan 2022)
39. <https://www.mindat.org/photo-751082.html> (Accessed 21 Jan 2022)
40. Gibbs GV, Rosso KM, Teter DM, Boisen MB Jr, Bukowski MST (1999) Model structures and properties of the electron density distribution for low quartz at pressure: a study of the SiO bond. *J Mol Struct* 485–486:13–25
41. Smyth JR (1989) Electrostatic characterization of oxygen sites in minerals. *Geochim Cosmochim Acta* 53:1101–1110
42. Cohen RE (1994) *Silica*. Mineralogical Society, Washington, p 369
43. Prencipe M, Nestola F (2007) Minerals at high pressure. Mechanics of compression from quantum mechanical calculations in a case study: the beryl ($\text{Al}_4\text{Be}_6\text{Si}_{12}\text{O}_{36}$). *Phys Chem Miner* 30:471–479
44. Prencipe M, Tribaudino M, Nestola F (2002) Charge density analysis of spodumene ($\text{LiAlSi}_2\text{O}_6$) from ab initio Hartree-Fock calculations. *Phys Chem Miner* 30:606–614
45. Harrison WA (1978) Is silicon dioxide covalent or ionic? In: Pantelides ST (ed) *The Physics of SiO₂ and its interfaces*, p. 105 Chapter 2. Pergamon Press, New York
46. Stewart RF, Whitehead MA, Donnay G (1980) The ionicity of the Si-O bond in low quartz. *Am Min* 65:324–326
47. Gibbs GV, Wallace AF, Cox DF, Downs RT, Ross NL, Rosso KM (2009) Bonded interactions in silica polymorphs, silicates, and siloxane molecules. *Am Miner* 94:1085–1102
48. Pauling L (1939) *The nature of the chemical bond*. Cornell University Press, Ithaca
49. Sanders MJ, Leslie M, Catlow CRA (1984) Interatomic potentials for SiO₂. *J Chem Soc Chem Commun*. <https://doi.org/10.1039/c39840001271>
50. Jackson MD, Gordon RG (1988) MEG investigation of low pressure silica—Shell model for polarization. *Phys Chem Miner* 16:212–220
51. Burnham CW (1990) The ionic model: perceptions and realities in mineralogy. *Am Miner* 73:443–463
52. Phillips JC (1970) Ionicity of the chemical bond in crystals. *Rev Mod Phys* 42:317–356
53. Vempati CS, Jacobs PWM (1983) Crystal potentials for alpha-quartz. *Radiat Eff Defects Solids* 73:285–289
54. Schnöckel H (1978) IR spectroscopic detection of molecular SiO₂. *Angew Chem Int Ed* 17:616–617
55. Schnöckel H (1996) In: Corriu R, Jutzi P (eds) *Tailor-made silicon-oxygen compounds: from molecules to materials*. Vieweg, Braunschweig, pp 131–140
56. Maier G, Reisenauer HP, Egenolf H, Glatthaar J (2003) Investigations on the reactivity of atomic silicon: a playground for matrix isolation spectroscopy. In: Jutzi P and Schubert U (eds) *Silicon chemistry: from the atom to extended systems*. Wiley-VCH Verlag, Weinheim, pp 4–19
57. Weil R (1931) Quelques observations concernant la structure du quartz. *Compte Rendu 1er Réunion de l'Institut d'Optique*: 2–11
58. Bambauer HU (1961) Spurenelementgehalte und γ -Farbzentren in quarzen aus zerrklüften der Schweizer Alpen. *Schweiz Min Petr Mitt* 41:335–369
59. Bambauer HU, Brunner GO, Laves F (1962) Wasserstoffgehalte in quarzen aus zerrklüften der Schweizer Alpen und deutung ihrer regionalen abhängigkeit. *Schweiz Min Petr Mitt* 42:221–236
60. Bambauer HU, Brunner GO, Laves F (1963) Merkmale des OH-spektrums alpiner quarze (3 μ -gebiet). *Schweiz Min Petr Mitt* 43:259–268
61. Hertweck B, Beran A, Niedermayr G (1998) IR-spektroskopische untersuchungen des OH-Gehaltes alpiner kluftquarze aus österreicherischen vorkommen. *Mitteilungen der österreichischen Mineralogischen Gesellschaft* 143:304–306
62. Friedlaender C (1951) Untersuchung über die eignung alpiner quarze für piezoelektrische zwecke. *Beiträge zur geologie der Schweiz, Geotechnische Serie, Lieferung* 29, 98 S
63. Roedder E (1981) Origin of fluid inclusions and changes that occur after trapping. *Mineralogical Association of Canada, Short course handbook* 6:101–137
64. Van den Kerkhof AM, Hein UF (2001) Fluid inclusion petrography 55:27–47
65. Roedder E (1984) Fluid inclusions. *Reviews in Mineralogy*, 12, Mineralogical Society of America, Chantilly, Virginia, USA, pp 645
66. Shepherd T, Rankin AH, Alderton DHM (1985) A practical guide to fluid inclusion studies. Blackie, Glasgow, p 239
67. Leeder O, Thomas R, Klemm W (1987) *Einschlüsse in ineralen*. VEB Deutscher Grundstoffverlag, Leipzig
68. Tasev G, Serafimovski T, Dolenc M, Rogan Šmuc N (2019) Contribution to understanding of ore fluids in the Zletovo mine based on fluid inclusion data. *RMZ-Mater Geoenviron* 66:75–86
69. Kostov RI, Bershov LV (1987) Systematics of paramagnetic electron-hole centres in natural quartz. *Izv Akad Nauk USSR. Ser Geol* 7:80–87 (in Russian)
70. Weil JA (1984) A review of electron spin spectroscopy and its application to the study of paramagnetic defects in crystalline quartz. *Phys Chem Miner* 10:149–165
71. Weil JA (1993) A review of the EPR spectroscopy of the point defects in a-quartz: The decade 1982–1992. In: Helms CR, Deal BE (eds) *Physics and chemistry of SiO₂ and the SiSiO₂ interface* 2. Plenum Press, New York, pp 131–144
72. Stevens-Kalceff MA, Phillips MR, Moon AR Kalceff W (2000) Cathodoluminescence microcharacterisation of silicon dioxide polymorphs. In: Pagel, M, Barbin V, Blanc P, Ohnenstetter D (eds) *Cathodoluminescence in geosciences*. Springer Verlag, Berlin, pp 193–224
73. Sjöberg S (1996) Silica in aqueous environments. *J Non Cryst Solids* 196:51–57
74. Exley C (1998) Silicon in life: a bioinorganic solution to bioorganic essentiality. *J Inorg Biochem* 69:139–144
75. Exley C (2015) A possible mechanism of biological silicification in plants. *Front Plant Sci* 6: Article 853
76. Choppin GR, Pathak P, Thakur P (2008) Polymerization and complexation behavior of silicic acid: a review. *Main Group Met Chem* 31:53–71
77. Iler RK (1979) In: *The chemistry of silica: solubility, polymerization, colloid and surface properties, and biochemistry*. John Wiley & Sons Inc, New York

78. Traexler KA, Utsunomiya S, Kersting AB, Ewing RC (2004) *Mat Res Soc Symp Proc*, 807
79. Karkanis P, Bar-Yosef O, Goldberg P, Weiner S (2000) Diagenesis in prehistoric caves: the use of minerals that form in situ to assess the completeness of the archaeological record. *J Archaeol Sci* 27:915–929
80. O'Brien MCM (1955) The structure of the colour centres in smoky quartz. *Proceedings of the Royal Society of London. Series A, Math Phys Sci* 231: 404–414
81. Lehmann G, Moore WJ (1966) Color center in amethyst quartz. *Science* 152:1061–1062
82. Maschmeyer D, Niemann K, Hake K, Lehmann G, Räuber A (1980) Two modified smoky quartz centres in natural citrine. *Phys Chem Miner* 6:145–156
83. Maschmeyer D, Lehmann G (1983) A trapped-hole center causing rose coloration of natural quartz. *Z Kristallogr* 163:181–186
84. Makreski P, Jovanovski G, Stafilov T, Boev B (2004) Minerals from Macedonia XII. The dependence of quartz and opal color on trace element composition- AAS, FT IR and micro Raman spectroscopy study. *Bull Chem Technol Maced* 23:171–184
85. Heaney PJ, Prewitt CT, Gibbs GV (1994) Physical behavior, geochemistry and materials applications. *Reviews in Mineralogy* 29, Mineralogical Society of America
86. Rossman GR. (1994) The colored varieties of the silica minerals. in *Silica: physical behavior, geochemistry and materials applications. Reviews in Mineralogy* 29, Mineralogical Society of America
87. Neumann E, Schmetzer K (1984) Mechanism of thermal conversion of colour and colour centres by heat treatment of amethyst. *N Jb Miner Monat* 272–282
88. Neumann E, Schmetzer K (1984) Farbe, farbursache und mechanismen der farbumwandlung von amethyst. *Z Dt Gemmol Ges* 33:35–42
89. Bank H (1976) Citrin. *Z Dt Gemmol Ges* 25:189–194
90. <https://www.irocks.com/minerals/specimen/29747> (Accessed 21 Jan 2022)
91. Blatt H, Christie JM (1963) Undulatory extinction in quartz of igneous and metamorphic rocks and its significance in provenance studies of sedimentary rocks. *J Sediment Res* 33:559–579
92. http://www.minsocam.org/msa/collectors_corner/article/mohs.htm (Accessed 21 Jan 2022)
93. Jeršek M, Jovanovski G, Boev B, Makreski P (2021) Intriguing minerals: corundum in the world of rubies and sapphires with special attention to Macedonian rubies. *ChemTexts* 7:19
94. Saigusa Y (2017) Chapter 5 – Quartz-based piezoelectric materials. In: Uchino Kenji (ed) *Advanced piezoelectric materials*. Woodhead publishing of materials, 2nd edition. Woodhead publishing, pp 197–233
95. (Accessed 21 Jan 2022)
96. Quartz. (1997) In: *Handbook of Mineralogy. III (Halides, Hydroxides, Oxides)*. Anthony JW, Bideaux RA, Bladh KW, Nichols MC (eds.), Mineralogical Society of America, Chantilly, VA
97. <https://geologyscience.com/minerals/quartz/> (Accessed 21 Jan 2022)
98. Hurlbut CS, Klein C (1985) *Manual of Mineralogy*, 20th edn. Wiley, New York
99. https://www.earthsciences.hku.hk/shmuseum/earth_mat_1_4.php (Accessed 21 Jan 2022)
100. <https://gemstagram.com/tourmalated-quartz-meanings-properties-and-benefits/> (Accessed 21 Jan 2022)
101. Simmons R, Ahsian N (2007) *The book of stones: Who they are and what they teach*, 4th ed. pp 336
102. Jovanovski G, Boev B, Makreski P, Najdoski M, Mladenovski G (2003) Minerals from Macedonia. XI. Silicate varieties and their localities – identification by FT IR spectroscopy. *Bull Chem Technol Macedonia* 22:111–141
103. O'Brien MCM (1955) The structure of the colour centres in smoky quartz. *Proceedings of the Royal Society of London. Series A, Math Phys Sci* 231:404–414
104. Partlow DP, Cohen AJ (1986) Optical studies of biaxial Al-related color centers in smoky quartz. *Am Miner* 71:589–598
105. Wiel JA (1975) The aluminium centers in α quartz. *Radiat Eff* 26:261–265
106. Nuttall RHD, Weil JA (1980) Two hydrogenic trapped-hole species in α -quartz. *Solid State Commun* 33:99–102
107. Nuttall RHD, Weil JA (1981) The magnetic properties of the oxygen-hole aluminium centers in crystalline SiO_2 . I. $[\text{AlO}_4]^{0-}$. *Can J Phys* 59:1696–1708
108. Meyer BK, Lohse F, Spaeth JM, Weil JA (1984) Optically detected magnetic resonance of the $(\text{AlO}_4)^{0-}$ centre in crystalline quartz. *J Phys C: Solid State Phys* 17:L31
109. Holden EF (1925) The cause of color in smoky quartz and amethyst. *Am Miner* 10:203–252
110. Fritsch E, Rossman GR (1988) An Update on color in gems. Part 2: Colors involving multiple atoms and color centers. *Gems Gemol* 24:3–15
111. Cox RT (1977) Optical absorption of the $d4$ ion Fe^{4+} in pleochroic amethyst quartz. *J Phys C10*:4631–4643
112. Gilg HA, Morteani G, Kostitsyn Y, Preinfalk C, Gatter I, Strieder AJ (2003) Genesis of amethyst geodes in basaltic rocks of the Serra Geral Formation (Ametista do Sul, Rio Grande do Sul, Brazil): a fluid inclusion, REE, oxygen, carbon, and Sr isotope study on basalt, quartz, and calcite. *Miner Deposita* 38:1009–1025
113. Jayaraman N (1939) The cause of colour of the blue quartzes of the charnockites of South India and of the champion gneiss and other related rocks of Mysore: *Proc. Indian Acad. Sci., Sect. A-9*, pp 265–285
114. Van Vultee J, Lietz JN (1955) Über die orientierten Verwachsungen von Rutil in Quarz. *N Jb Miner Abh* 87(3):389–415
115. Zolensky ME, Paces SPI, JB, (1988) Origin and significance of blue coloration in quartz from Llano rhyolite (Ilanite), north-central Llano Country, Texas. *Am Miner* 73:313–332
116. Bukanov VV, Markova GA (1969) The smoky and citrine color of natural quartz. *Dokl. Akad. Nauk SSSR. Earth Sci Sections* 187:115–117
117. Aines RD, Rossman GR (1986) Relationships between radiation damage and trace water in zircon, quartz, and topaz. *Am Miner* 71:1186–1193
118. Krefft GB (1975) Effects of high-temperature electrolysis on the coloration characteristics and OH-absorption bands in α -quartz. *Radiat Eff* 26:249–260
119. Nassau K, Prescott BE (1975) A reinterpretation of smoky quartz. *Phys Stat Sol* 29:659–663
120. Nassau K, Prescott BE (1977) Smoky, blue, greenish yellow, and other irradiation-related colors in quartz. *Mineral Mag* 4:301–312
121. Nassau K, Prescott BE (1977) A unique green quartz. *Am Miner* 62:589–590
122. Hurrell K, Johnson ML (2016) *Gemstones: a complete color reference for precious and semiprecious stones of the world*. Chartwell Books, New York
123. Applin K, Brian H (1987) Fibers of dumortierite in quartz. *Am Miner* 72:170–172
124. Goreva JS, Ma C, Rossman GR (2001) Fibrous nano-inclusions in massive rose quartz: the organ of rose coloration. *Am Miner* 86:466–472
125. Ma C, Goreva JS, Rossman GR (2002) Fibrous nano-inclusions in massive rose quartz: HRTEM and AEM investigations. *Am Miner* 87:269–276

126. Wright PM, Weil JA, Buch T, Anderson JH (1963) Titanium colour centres in rose quartz. *Nature* 197:246–248
127. Lehmann G, Bambauer HU (1973) Quarzkristalle und ihre Farben. *Angew Chem* 86:281–290
128. Schmetzer K, Krzemnicki M (2006) The orientation and symmetry of light spots and asterism in rose quartz spheres from Madagascar. *J Gemmol* 30:183–191
129. Killingback H (2008) The positions of light spots on rose quartz star spheres. *J Gemmol* 31:40–42
130. https://www.fabreminerals.com/search_show.php?SECTION=RSBR&CODE=TR66J0 (Accessed 21 Jan 2022)
131. Platonov AN, Sachanbiński M, Wróblewski P, Ignatov SI (1991) Rare varieties of green quartz from quartz-agate geodes in Lower Silesia, Poland. *Mineral Zh* 13:10–17 (in Russian)
132. <http://www.quartzpage.de/prasiolite.html> (Accessed 21 Jan 2022)
133. Bahman R, Parisa H (2021) “Herkimer diamond” quartz from North-western Iran. *J Gemmol* 37:567–569
134. <https://www.mindat.org/min-1877.html> (Accessed 21 Jan 2022)
135. Baldwin M (2003) Herkimer diamonds. *MAGS Explorer, Memphis Archaeological and Geological Society Youth Newsletter* 2(7):1–3
136. Strasser M (2007) “Herkimer quarze” aus der ehnbachklamm in zirl. *Tirol Lapis* 32:23–24
137. Smith CH (1952) Recent Herkimer “diamond” hunting. *Rocks Miner* 27:272–275
138. Lt. Bill, F. Francis (1953) The largest Herkimer “diamond”? *Rocks Miner* 28:26–27
139. Marshall BC (1954) A still larger Arkansas Herkimer “diamond.” *Rocks Miner* 29:360–361
140. <https://www.mindat.org/min-960.html> (Accessed 21 Jan 2022)
141. <https://www.mindat.org/photo-162457.html> (Accessed 21 Jan 2022)
142. <https://www.mindat.org/min-51.html> (Accessed 21 Jan 2022)
143. <https://www.flickr.com/photos/jsjgeology/44632240655/> (Accessed 21 Jan 2022)
144. Barasanov GP, Yakovleva ME (1981) Mineralogical investigations of some precious and semi-precious varieties of cryptocrystalline silica. *USSR Academy of Sciences, In New Mineral Data*, p 29
145. Heflik W, Kwieceńska B, Natkaniec-Nowak L (1989) Colour of chrysoprase in light of mineralogical studies. *Austral Gemmol* 17(43–46):58–59
146. Faust GT (1966) The hydrous nickel-magnesium silicates—the garnierite group. *Am Mineral* 51:33–36
147. Sachanbinski M, Janeczek J, Platonov A, Rietmeijer FJM (2001) The origin of colour of chrysoprase from Szklary (Poland) and Sarykul Boldy (Kazakhstan). *N Jb Miner Abh* 177:61–76
148. Frondel C (1962) The system of mineralogy of James Dwight Dana and Edward Salisbury Dana. Vol 3, 7th edition, *Silica Minerals*. John Wiley and Sons, New York, pp 334
149. Bons PD (2001) The formation of large quartz veins by rapid ascent of fluids in mobile hydro fractures. *Tectonophysics* 336:1–17
150. Semaw S, Renne P, Harris JWK, Feibel CS, Bernor RL, Fesseha N, Mowbray K (1997) 2.5-million-year-old stone tools from Gona. *Ethiopia Nat* 385:333–336
151. Nathan Y, Segal I, Delage C (1999) Geochemical characterization of cherts from northern Israel (western Galilee). *Isr J Earth Sci* 48:235–245
152. Barkai R, Gopher A, La Porta PC (2002) Palaeolithic landscape of extraction: flint surface quarries and workshops at Mt Pua, Israel. *Antiquity* 76:672–680
153. Vermeersch PM, Paulissen E, Van Peer P (1990) Palaeolithic chert exploitation in the limestone stretch of the Egyptian Nile Valley. *Afr Archaeol Rev* 8:77–102
154. Nachev C, Kanchev K (1978) Investigation of the chert material from the archaeological excavations: problems and purposes (Interdisciplinary studies) 2:81–89 (in Bulgarian)
155. Nachev IK, Nachev CI (1989), Distribution and evolution of siliceous rocks in Bulgaria. In: Hein JR, Obradović J (eds) *Siliceous deposits of the Tethys and Pacific Regions*. Springer-Verlag, New York, pp 81–92
156. Gurova M, Nachev C (2008) Formal early neolithic flint toolkits: archeological and sedimentological aspects Proceedings of the international conference of Geoarchaeology and Archaeomineralogy, Sofia, Bulgaria, pp 29–35
157. Olofsson A, Rodushkin I (2011) Provenancing flint artefacts with ICP-MS using REE signatures and Pb isotopes as discriminants: preliminary results of a case study from Northern Sweden. *Archaeometry* 53. Oxford
158. [https://en.wikipedia.org/wiki/Heliotrope_\(mineral\)](https://en.wikipedia.org/wiki/Heliotrope_(mineral)) (Accessed 21 Jan 2022)
159. <https://pixabay.com/photos/rock-mineral-cristobalite-nature-4135390/> (Accessed 10 Jan 2021)
160. Downs RT, Palmer DC (1994) The pressure behavior of a cristobalite. *Am Miner* 79:9–14
161. Leadbetter AJ, Wright AF (1976) The α - β transition in the cristobalite phases of SiO₂ and AlPO₄ I. X-ray studies. *Philos Mag* 33:105–112
162. <https://www.mindat.org/min-4015.html> (Accessed 21 Jan 2022)
163. https://commons.wikimedia.org/wiki/File:Tridymite_aggregate_-_Ochtendung,_Eifel,_Germany.jpg (Accessed 21 Jan 2022)
164. Konnert JH, Appleman DE (1978) Crystal structure of low tridymite. *Acta Crystallogr B* 34:391–493
165. Podwórny J, Zawada J (2010) The structure of low-temperature tridymite in silica refractories. *Solid State Phenom* 163:187–190
166. <https://www.mindat.org/min-3004.html> (Accessed 21 Jan 2022)
167. Burg SL, Parnell AJ (2018) Self-assembling structural colour in nature. *J Condens Matter Phys* 30: Article 413001
168. <https://www.uniqueopals.ch/opal-play-of-colour.htm> (Accessed 21 Jan 2022)
169. https://www.itp.uni-hannover.de/fileadmin/itp/emeritus/zawischa/static_html/scattering.html (Accessed 21 Jan 2022)
170. Jovanovski G, Boev B, Makreski P (2012) Minerals from the Republic of Macedonia with an introduction to mineralogy, *Macedonian Academy of Sciences and Arts, Skopje*
171. Rudnick RL, Gao S (2003) 3.01 Composition of the continental crust. *Treatise On Geochemistry, Volume 3: The Crust*. Elsevier Ltd. 1st Edition, 1–64
172. Wangen M, Munz IA (2004) Formation of quartz veins by local dissolution and transport of silica. *Chem Geol* 209:179–192
173. Pati JK, Patel SC, Pruseth KL, Malviya VP, Arima M, Raju S, Pati P, Prakash K (2007) Geology and geochemistry of giant quartz veins from the Bundelkhand Craton, Central India and their implications. *J Earth Syst Sci* 116:497–510
174. Vinx R (2015) *Gesteinsbestimmung im Gelände*. Springer Verlag, Heidelberg, p 480
175. Sawyer EW, Robin P-YF (1986) The subsolidus segregation of layer-parallel quartz-feldspar veins in greenschist to upper amphibolite facies metasediments. *J Metamorph Geol* 4:237–260
176. Heddle MF (1901) *Mineralogy of Scotland*. Edinburgh 2:110–112
177. Beljankin DS, Petrov VP (1938) Occurrence of cristobalite in a sedimentary rock. *Am Miner* 23:153–155
178. Darling RS, Chou I-M, Bodnara RJ (1997) Occurrence of metastable cristobalite in high-pressure garnet. *Science* 276(5309):91–93
179. <https://www.britannica.com/science/tridymite> (Accessed 21 Jan 2022)

180. Lakdawalla E (2015) Curiosity stories from AGU: the fortuitous find of a puzzling mineral on Mars, and a gap in Gale's history. The Planetary Society
181. Mitchell RS, Tufts S (1973) Wood opal—a tridymite-like mineral. *Am Miner* 58:717–720
182. Sanders JV (1975) Microstructure and crystallinity of gem opals. *Am Miner* 60:749–757
183. Stoiber RE, Tolman C, Butler RD (1945) Geology of quartz crystal deposits. *Am Miner* 30:219–229
184. <https://www.worldatlas.com/articles/top-15-quartz-exporting-countries.html> (Accessed 21 Jan 2022)
185. <http://www.bonzele.com/c/a?a=p&p=299008&cmd=sp&op=767> (Accessed 21 Jan 2022)
186. Roberts RJ, Irving EM (1957) Quartz deposits Guatemala: in Mineral deposits of Central America. *Bull US Geol Surv* 1034:161–169
187. <https://www.mindat.org/locentries.php?p=14314&m=3337> (Accessed 21 Jan 2022)
188. <https://www.flickr.com/photos/42200412@N03/51397645711> (Accessed 21 Jan 2022)
189. <https://www.mindat.org/photo-34654.html> (Accessed 21 Jan 2022)
190. <https://www.geologyin.com/2020/04/worlds-largest-quartz-crystal-cluster.html> (Accessed 21 Jan 2022)
191. <https://www.flickr.com/photos/squeakymarmot/134532956/in/set-72057594116134496/> (Accessed 21 Jan 2022)
192. Platonov AN, Szuszkiewicz A (2016) Green to blue-green quartz from Rakowice Wielkie (Sudetes, south-western Poland)—a re-examination of prasiolite-related colour varieties of quartz. *Mineralogia* 46:19–28
193. <https://www.mindat.org/locentries.php?p=2147&m=3337> (Accessed 21 Jan 2022)
194. Blažev K (1991) Mineralogy of the raw materials of Macedonia and their economic importance, PhD thesis, Ss Cyril and Methodius University in Skopje **(in Macedonian)**
195. Blažev K, Doneva B, Dimov G, Delipetrev M (2017) Secondary silica raw materials in quaternary continental formations, X Expert counseling with international participation Podex-Povex '17, 03–05 November 2017, Ohrid, Macedonia, Book of Abstracts 267–271 **(in Macedonian)**
196. Filipovski B (1974) Geologic composition and ore wealth of SR Macedonia. Scientifically popular literature-book, publishing community at NIP New Macedonia, Skopje, 1–139 **(in Macedonian)**
197. Blažev K (1981) Report on the occurrences of piezo-optical quartz in the area of villages Budinarci-Mitrasinci. Geological part of the company Opalit-Chešinovo
198. Blažev K, Šijakova-Ivanova T, Stojanova V, Doneva B (2016) Piezooptic quartz localities Budinarci-Mitrasinci. IX Professional conference Podeks-Poveks'16 with international participation, 11–13 Nov 2016, Strumica, Macedonia, Book of Abstracts 41–44 **(in Macedonian)**
199. Adjigogov L (1971) Final report for regional investigation of quartzite in Vardar zone, Geological survey of the Republic of Macedonia
200. Blažev K, Doneva B, Dimov G, Delipetrev M, Delipetrov T (2017) Types of silica raw materials on the territory of the Republic of Macedonia. 7-th Balkan Mining Congress, 11–13 Oct 2017, Prijedor, Bosnia and Herzegovina, Book of Abstracts 33–38
201. Blažev K, Doneva B, Dimov G, Panov Z, Delipetrov T, Delipetrov M (2018) Geomechanical characteristics of quartzites as construction material and their potentiality in the Republic of Macedonia. VIII International Geomechanics Conference, 2–6 July 2018, Varna, Bulgaria, Proceedings 3–9
202. Blažev K, Doneva B, Dimov G, Delipetrev M, Delipetrov T, Panov Z (2017) Physical and mechanical characteristics of the secondary quartzites from the deposit Peshter in the Republic of Macedonia. XIV International Conference of the Open and Underwater Mining of Minerals, 3–7 July 2017, Varna, Bulgaria, Book of Abstracts 46–51.
203. Barić L (1964) Mineralogy of the Crni Kamen locality near the village Alinci in Macedonia, Mineralogic-Petrographic Museum, Zagreb, 23–30 **(in German)**
204. Šijakova-Ivanova T (1989) Crystallographic and crystal chemistry characteristics of the non-metallic minerals from scarn ore deposit Sasa. M. Sc. Thesis, Faculty of Mining and Geology, Belgrade **(in Serbian)**
205. Aleksandrov M, Serafimovski T (1993) The association of the elements in the lead–zinc locality Golema Reka (Sasa). *Geologica Macedonica* 6:3–14 **(in Macedonian)**
206. Denkovski G, (1974) The mineral genesis of the vein 2 in the Dobrevno mine, VIII Congress of Geologists of Yugoslavia, Bled, Book of Papers, 41–54 **(in Macedonian)**
207. Serafimovski T (1993) The structure and metalogenetic characteristics of the Lecce-Chalcidici zone. Faculty Mining Geol 2:328
208. Rakičević T, Dumurdžanov N, Petkovski P (1976) The Interpretation of the basic geological map of the Republic of Macedonia for the Štip Sheet. Geological survey of Macedonia **(in Macedonian)**
209. Serafimovski T (1990) Metalogenetic characteristics of the Lecce-Chalcidici zone, Ph.D. Thesis, Faculty of Mining and Geology, Štip **(in Macedonian)**
210. Dumurdžanov N, Hristov S, Pavlovski B, Ivanova V (1976) The interpretation of the basic geological map of the Republic of Macedonia for sheet K-34–104 Vitolište and K-34–116 Kajmakčalan, 61, Geological survey of Macedonia **(in Macedonian)**
211. <https://sciencing.com/differences-between-minerals-calcite-quartz-8447374.html> (Accessed 21 Jan 2022)
212. <https://uniquecrystalminerals.com/quartz-applications/> (Accessed 21 Jan 2022)
213. Aasly K, Malvik T, Myrhaug EH (2007) A review of previous work on important properties of quartz for FeSI and Si metal production. Innovations in ferro alloy industry, New Delhi, India, INFOCON XI, pp 393–401
214. Jamo HU (2016) Structural analysis and surface morphology of quartz. *Bayero J Pure Appl Sci* 9:230–233
215. Curie J, Curie P (1880) Développement, par pression, de l'électricité polaire dans les cristaux hémihédres à faces inclinées. *CR Acad Sci* 91:294–295
216. Curie J, Curie P (1880) Sur l'électricité polaire dans les cristaux hémihédres à faces inclinées. *C R Acad Sci* 91:383–386
217. Lippmann G (1881) Principe de la conservation de l'électricité. *Ann Chim Phys* 24:145–178
218. Katzir S (2003) The discovery of the piezoelectric effect. *Arch Hist Exact Sci* 57:61–91
219. <https://everythingexplained.today/Piezoelectricity/> (Accessed 21 Jan 2022)
220. Lombardi M (2008) The accuracy and stability of quartz watches. *Horol J* 57–59.
221. <https://www.hodinkee.com/articles/four-revolutions-quartz-revolution> (Accessed 21 Jan 2022)
222. Bottom VE (1981). A history of the quartz crystal industry in the USA. In: Proceeding of 35th annual frequency control symposium 3–12
223. Johnson GR (2004). History of the industrial production and technical development of single crystal cultured quartz. In: Proceedings of the IEEE international frequency control symposium and exposition, pp 35–45

224. <https://pubs.usgs.gov/periodicals/mcs2021/mcs2021.pdf> (Accessed 21 Jan 2022)
225. Iwasaki F, Iwasaki H (2002) Historical review of quartz crystal growth. *J Cryst Growth* 237–239:820–827
226. https://it.wikipedia.org/wiki/Giorgio_Spezia (Accessed 21 Jan 2022)
227. Spezia G (1909) Sull' accrescimento del quarzo. *Atti Accad Sci Torino* 44:95–109
228. Spezia G (1905) La pressione e' chimicamente inattive nella solubilita e riecostituzione del quarzo. *Atti Accad Sci Torino* 40:254–262
229. https://de.wikipedia.org/wiki/Richard_Nacken (Accessed 21 Jan 2022)
230. Nacken R (1950) Die hydrothermale mineralsynthese als grundlage zur zuchtung von quarzkristallen. *Chemiker-Ztg Jahrg* 50:745–749
231. Feigelson RS (2004). Contributors. In: Feigelson RS (eds) 50 years progress in crystal growth. Elsevier, xxvi.
232. Buehler E, Walker AC (1949) Growing quartz crystals. *Sci Monthly* 69:148–155
233. Brown CS, Kell RC, Thomas LA, Wooster N, Wooster WA (1952) The growth and properties of large crystals of synthetic quartz. *Min Mag* 29:858–874
234. Feigelson RS (2015). Crystal growth through the ages. In: Handbook of crystal growth (2nd Edition), Elsevier 1–83
235. Bhat HL (2014). Growth from liquid solutions. In: Introduction to crystal growth (1st Edition), CRC Press 183–240
236. Kolis JW, Korzenski MB (2007) Synthesis of inorganic solids. In: Jessop PG, Leitner W (eds) Chemical synthesis using supercritical fluids. Wiley, Hoboken, pp 213–242
237. Byrappa K, Yoshimura M (2001) Apparatus. Handbook of hydrothermal technology—a technology for crystal growth and materials processing. Elsevier, pp 82–160
238. Laudise RA, Barns RL (1988) Perfection of quartz and its connection to crystal growth. *IEEE Trans Ultrason Ferroelectr Freq Control* 35:277–287
239. Anthony AM, Collongues R (1972) Modern methods of growing single crystals of high-melting-point oxides. In: Hagenmuller P (ed) Preparative methods in solid state chemistry. Elsevier, pp 147–249
240. King JC, Ballman AA, Laudise RA (1962) Improvement of the mechanical Q of quartz by the addition of impurities to the growth solution. *J Phys Chem Sol* 23:1019–1021
241. Laudise RA, Nielsen JW (1961) Hydrothermal crystal growth. *Solid State Phys* 12:149–222
242. Nagy J, Tarján I (1957) Über die züchtung künstlicher quarzkristalle. *Acta Phys Acad Sci Hun* 6:485–488
243. Brown CS, Kell RC, Middleton P, Thomas LA (1955) Influence of impurities on the growth of quartz crystals from flint and quartzite. *Nature* 175:602–603
244. Brown CS, Kell RC, Thomas LA, Wooster N, Wooster WA (1951) Growth of large quartz crystals. *Nature* 167:940–941
245. <http://www.theimage.com/newgems/synthetic/syntheticanimat e4.html> (Accessed 21 Jan 2022)
246. Regreny A (1973) Recristallisation hydrothermale du quartz et caractérisation en vue des applications radioélectriques. *Ann Télécommun* 28:111–122
247. Tareen JAK, Basavalingu B, Shankara MA, Fazeli AR (1986) A simple hydrothermal cell for synthesis at moderate temperatures and pressures. *Bull Mater Sci* 8:543–546
248. Regreny A, Aumont R (1970) Recristallisation hydrothermale du quartz. *Ann Télécommun* 25:294–306
249. Walker AC (1953) Hydrothermal synthesis of quartz crystals. *J Am Ceram Soc* 36:250–256
250. <https://www.nanoquarzwafers.com/products/fused-silica-wafer/> (Accessed 21 Jan 2022)
251. https://en.wikipedia.org/wiki/Fused_quartz (Accessed 21 Jan 2022)
252. Kitamura R, Laurent P, Miroslaw J (2007) Optical constants of silica glass from extreme ultraviolet to far infrared at near room temperatures. *Appl Opt* 46:8118–8133
253. Salem JA (2013) Transparent armor ceramics as spacecraft windows. *J Am Ceram Soc* 96:281–289

Publisher's Note Springer Nature remains neutral with regard to jurisdictional claims in published maps and institutional affiliations.